SOIL CONTAMINANT MAPPING AND PREDICTION OF SEDIMENT YIELD AT AN ABANDONED URANIUM MINE

DRAFT Plan B Technical Report

Prepared by

Aaron Orechwa, P.E.
Department of Civil and Environmental Engineering
Colorado State University

In partial fulfillment of the
M.S. Plan B Degree Requirements
Adviser: Dr. Pierre Julien

October 5, 2015

TABLE OF CONTENTS

LIST OF TABLES

LIST OF FIGURES

ABSTRACT

The legacy of uranium mining in the Western U.S. is widespread and will take many years to address. Mining during the Cold War era uranium boom at the Riley Pass Abandoned Uranium Mine in the Custer National Forest, located in Harding County, South Dakota, is a significant part of South Dakota's legacy uranium mining history. Under the historical general mining laws of that era, unrestricted strip mining took place at this site with no requirements for reclamation. Ten mine-affected study areas within the Riley Pass site are approved by the U.S. Environmental Protection Agency (EPA) for non-time critical removal actions under the Comprehensive Environmental Response, Compensation, and Liability Act (CERCLA). Site specific risk-based cleanup action levels for surface soil are established for select heavy metals and radionuclides of concern. This case study presents innovative monitoring and mapping techniques for contaminants in soil to predict the spatial extent of concentrations of these contaminants within surface soils at the site. Statistical evaluations used in sizing sampling grids, evaluation of the feasibility of utilizing double sampling methods versus simple random sampling, and geostatistical mapping techniques used to establish cleanup boundaries are presented in this paper.

The degradation of land caused by strip mining is a multi-faceted phenomena, where the effects seen are caused by deterioration of the land surface by accelerated removal of soil, progressive alteration of soil properties, and loss of vegetative cover of the soil. Drainages from the site have been subject to severe erosion and sedimentation since mining operations seized in the early 1960s. The second objective of this paper is to predict the soil losses and associated sediment yields of the five primary watersheds at the largest study area of the site. This paper presents the results of a soil erosion analysis using a Geographic Information System (GIS) application of the Revised Universal Soil Loss Equation (RUSLE) to predict sediment yield and specific degradation rates within mining-impacted watersheds. Data on removal of pond sediment from existing sediment pond cleanout construction were used to validate the model results. Using available soil contaminant data, a GIS analysis approach was performed to estimate contaminant load and predict the resultant sediment concentrations of arsenic, radium-226, and uranium at downstream locations of each watershed. Sediment data collected during previous studies at the site were used to validate the estimated sediment contaminant concentrations. Results of the study showed the RUSLE model produced accurate estimates of sediment yield, specific degradation, and sediment contaminant concentrations when compared with available site data. The information presented in this case study can be used to assess priority cleanup action areas and as an engineering application for sizing of future sediment containment facilities at the study area.

1.0 INTRODUCTION

1.1 OVERVIEW

During the Cold War, many private companies operated uranium mines in the western U.S. under contracts with the U.S. government, removing 4 million tons of ore that went into making nuclear weapons and fuel and leaving a legacy of radiological and chemical hazards. Currently, 15,000 sites are associated with uranium extraction in the U.S. Environmental Protection Agency (EPA) Uranium Location Database (EPA, 2006). Ore was extracted by strip mining at many sites. Protected under the General Mining Laws, including the Atomic Energy Act of 1946 and Public Law 357, strip mining did not require environmental restoration or post-mining responsibility (USFS, 2006). This case study focuses on the Riley Pass Abandoned Uranium Mines (Riley Pass) located in the North Cave Hills complex in northwestern South Dakota. The strip mining at Riley Pass involved removal of uranium-bearing lignite coal beds in an area that already had geologically rapid retreat. This mining during the 1950s and early 1960s at Riley Pass is a significant part of South Dakota's uranium mining history; however, the legacy of these mining operations have left unintended and negative pollution that has impaired the surrounding environment to above acceptable human health and ecological risk levels.

Mining operations may introduce large volumes of sediment directly into natural streams, and the mine dumps and spoils often continue to erode by natural rainfall for many years after the mining operations have ceased (Julien, 2010). Surface mining or "strip mining" makes the impact on the environment especially acute and can severely erode the soil. Land degradation from strip mining is a global environmental crisis, threatening watersheds and surrounding environmental media. Pollutants commonly found at surface uranium mines include heavy metals and radionuclides that have the potential to impair the quality of surface water and groundwater in the vicinity of the mine site. These potential impacts are increased when the contaminated soils or waste materials are eroded and washed into water bodies (EPA 2000). Pollutants at a mine site including metals, nitrates, sulfates, and radionuclides have the potential, once dissolved, to contaminate aquatic and biological systems within the area of the mine for many years after operations have ceased.

This study focuses on mapping contaminant concentrations in soils, soil erosion modeling, and predicting sediment yield and erosion rates at the Riley Pass study area. The methods presented in this report rely heavily on Geographic Information Systems (GIS) for multiple facets of the analyses. The following section presents a detailed account of the site history.

1.2 BACKGROUND

Uranium exploration began in the North Cave Hills in 1954, when the Atomic Energy Commission recorded high radiation anomalies over the North Cave Hills (Curtiss, 1955; Stone et al., 2009). The first claims were staked in August 15, 1954; extensive mining started in the early 1960s in an effort to supply contracts for uranium, but all mining ceased in 1964. Riley Pass is part of the North Cave Hills complex contained within the Sioux Ranger District, Custer National Forest, in Harding County, South Dakota, falling within Region 1 jurisdiction of the United States Forest Service (USFS). The site is located 25 miles north of Buffalo, South Dakota. The nearest town is Ludlow, South Dakota, which lies 5 miles to the east. A small fraction of the site is situated on private land (USFS 2007). The Riley Pass site consists of 10 study areas with more than 316 acres of mine-impacted land referred to as Bluff A, Bluff B, Bluff CDE, Bluff F, Bluff G, Bluff H, Bluff I, Bluff J, Bluff K, and Bluff L.

The site includes steep-sided and flat-topped buttes that are rimmed with sandstone cliffs. From a geomorphic perspective, this area contains evidence of geologically rapid retreat (Stone et al., 2007). The climate in the region is intercontinental arid characterized by warm dry summers and cool dry winters, with an average precipitation of 12 inches per year. Snowfall does not typically contribute to the total precipitation amount. The uranium mines located in this region were lignite mines located on the tops of the buttes. Mining features include bluffs, overburden piles (spoils), and hazardous erosional openings and highwalls. Samples of spoils materials have been characterized as sandy clay and clayey sand. Within the North Cave Hills, documented mine sites, spoils, and exploration activities cover almost 1,000 acres. However, the estimated disturbed areas within the Riley Pass site include 300 acres of highwalls, pit floors, and spoils piles. Spoils were pushed over the edges of the buttes onto the steep slopes below the rimrocks during mining. Additional spoils have been deposited on these slopes by erosion.

Because of the predominant soil type present — sandy clay and silty clay — soil piping and tunneling with occasional sink holes are present. Piping and large gullies are most prevalent in areas where the overburden was placed along or below the rimrocks. Some of the pipes that have formed are 10 feet to 15 feet in diameter, and gullies up to 25 feet in depth have formed in places. The mined pit floors are generally at or near bedrock. Some spoils have been placed along the edges that erode to the land below Bluff B. Small, shallow ponds have formed in some of the areas, creating small retention basins, which during snowmelt and small storm events assist in controlling some of the surface water erosion. Water from these ponds most likely evaporates or seeps through the bedrock during the summer.

Under the General Mining Laws, per the Atomic Energy Act of 1946 and Public Law 357, unrestricted strip mining took place within the North Cave Hills during the 1950s and 1960s. The strip mining involved removal of uranium-bearing lignite coal beds, with no requirements for environmental restoration or for establishing post-mining responsibility (USFS, 2006). The nature of mining that took place resulted in acute environmental degradation and has eroded the soils and affected drainages and water supplies. Numerous investigations conducted at the site have shown impacts of heavy metals and radionuclides releases associated with the mining.

1.3 PROBLEM STATEMENT

The Riley Pass Abandoned Uranium Mine is located in Harding County, South Dakota, within the Custer-Gallatin National Forest. The total mine affected area identified by Tetra Tech Inc. (2015) is 316 acres. This paper focuses on the largest area, Bluff B, which also has the worst erosion and sedimentation issues and most widespread contamination. The Bluff B study area shown in Figure 1 encompasses approximately 153 acres of spoils piles (overburden), highwalls, and open pits. Bluff B is located in parts of Township 22 North, Range 5 East, Sections 22,23,26 and 27. A significant historical pioneer wagon route during the 1890s is located within approximately 500 feet of the study area. Bluff B is the largest study area at Riley Pass, and the waste materials (spoils and overburden) have been a major source of sedimentation to Pete's Creek to the east of Bluff B and Schleichart Draw to the southeast, shown in Figure 1. A majority of the bluff is either barren or sparsely vegetated and shows signs of severe erosion by wind and surface water. Major sources of erosion and sediment loadings at the study area include open pit areas, waste rock and overburden piles, tailings piles, haul and access roads, ore stockpiles and many others (EPA, 2000). Sediment from the east half of the site is currently being carried approximately 0.75 mile and deposited on the main access road to Riley Pass and the adjoining private property. The USFS records from 1931 through 1983 report average annual precipitation at Ludlow, South Dakota, of 14.8 inches (375 millimeters [mm]) (USFS, 2004). Approximately 73 percent (10.8 inches) of this precipitation appears in the form of rain during May through September.

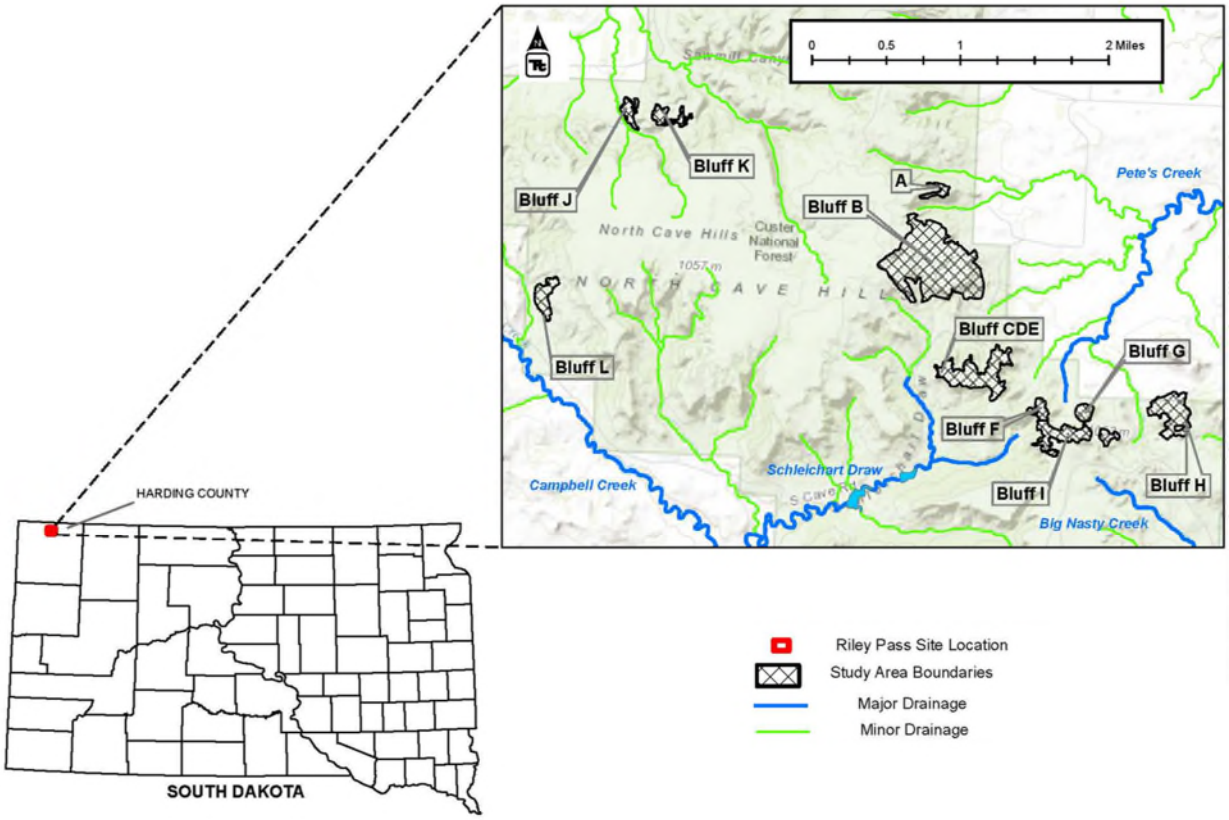

Figure 1 Site Location Map

Mining operations in the region completely stopped in 1964; however, erosion and sedimentation continued within the vicinity of Bluff B until the present. In 1989, the USFS constructed three sediment ponds to contain mine sediment from being directly transported out of the drainages of Bluff B. These ponds were installed and maintained to prevent sediment entering Pete's Creek and Schleichart Draw. The ponds were designed with drop outlet structures that allow for sediment-laden water to remain in the ponds until the water reaches the outlet level (USFS, 2004). Four of primary drainages from Bluff B flow into Pete's Creek drainage basin; two sediment ponds were placed within these tributaries to reduce the sediment load into the creek. Two drainage areas from Bluff B remain uncontrolled, allowing for sediment discharge directly into Pete's Creek during major storms. Additionally, the third sediment pond was installed at a major southern drainage from Bluff B that flows into Schleichart Draw. As a result of the amount of sediment eroding from the site, frequent maintenance of the sedimentation ponds is required. The sediment ponds have been cleaned out completely on numerous occasions, allowing for direct measurement of sediment volume for given periods of time. Additionally, geotechnical and geochemical characterizations have been performed on the material in the ponds a number of times.

A study by South Dakota School of Mines and Technology (SDSMT) for the United States Department of Agriculture (USDA) was conducted in 2007 (Stone et al., 2007). The primary objective of this study was to assess the extent of heavy metal and radionuclide contamination found on private property attributed to historical mining operations within the North Cave Hills complex. The study consisted of a large-scale evaluation of concentrations in soils, sediment, groundwater, and surface water for the target analytes of concern on the site and within the vicinity of the site on private property. Previous investigations established background concentrations target analytes in soil for both undisturbed areas and the same stratigraphic interval of the mined lignite (Portage, 2006). The 2007 SDSMT study concluded that the highest contaminant concentrations were generally limited to Pete's Creek drainage for up to 15 to 20 kilometers (km) downstream from source areas (Bluff B) before contaminant concentrations were less than 3 times background. The location of Pete's Creek is shown in Figure 1. One of the findings and recommendations of the Stone et al. (2007) study included design of a proposed sedimentation pond to be located below the northeastern spoils of Bluff B (referred to as "East" watershed for this paper). Currently, no sediment pond is located in this area, and this region is a major area for the transport of contaminated spoils and sediments into the downstream area.

There are five primary watershed areas at Bluff B that transport contaminated runoff and sediment into the surrounding environment. Sediment control structures are in place at three of these watersheds that reduce the contaminated media from entering these areas to an extent. The purpose of this study is to utilize existing data and other available information to perform soil loss modeling and predict the sediment yield and sediment contaminant concentrations that leave each of the five watersheds of Bluff B. This information can be used to make recommendations for engineering applications, including proposed cleanout scheduling and sedimentation pond design and size. Additionally, the results of this study can be applied to identify and focus areas of concern for future remedial actions necessary to reduce further contamination into the surrounding environment and downstream areas. Coincidentally, site-wide data are available to validate the model results and calibrate the model if necessary. The next section presents the objectives of this study.

1.4 STUDY OBJECTIVES

This paper presents a broad approach to evaluating a variety of factors pertaining to and assessing the risks from mine impacted land that is contaminated with heavy metals and radionuclides and is subject to significant hydrological impacts by erosion from wind and natural rainfall. The methods and results presented in this paper rely heavily on the application of GIS for soil contaminant mapping , drainage network processing, hydraulic modeling, and soil erosion modeling. The objectives of this study are as follows:

- Present the findings from a detailed literature review on uranium mine contamination, environmental monitoring, erosion, and GIS applications related to this study.
- Using terrain processing tools in GIS and available digital elevation mapping (DEM) data sets, delineate stream networks and watersheds for Bluff B.
- Estimate the annual gross erosion from each watershed in tons/year using a GIS application of the Revised Universal Soil Loss Equation (RUSLE).
- Calculate the sediment delivery ratio, sediment yield, and specific degradation of each watershed and compare to database of reservoir sedimentation field measurements from U.S. reservoirs and validate with site data.
- Using soil contaminant mapping information, estimate the mass and concentration of arsenic, uranium, and radium-226 that is being transported off site from each of the watersheds and validate with site data.

2.0 LITERATURE REVIEW

A comprehensive literature review was conducted on the subjects of interest to meet the project objectives. A summary of the literature review findings is provided in this chapter.

2.1 URANIUM MINE CONTAMINATION AND REMEDIATION

Between the 1940s and 1990s, thousands of uranium mines operated primarily in the western continental United States, leaving a legacy of potential radiological and chemical hazards. There are an estimated 15,000 locations associated with uranium in the EPA database, of which 4,000 of these have documented production (EPA 2006). Figure 2 shows the locations in the western U.S. The lasting impacts of these abandoned uranium mines present a significant risk to human health and the environment associated with the potential radiological and chemical hazards remaining at these sites. These sites have the potential to impair watersheds and become health hazards if not properly reclaimed and abandoned.

Mining is a disruptive activity involving physical disturbance of the earth's surface to gain access to the ore, re3moving and processing the ore, and depositing wastes generated by ore processing (Robertson, 1996). The initial step of the mining and mineral processing operations is the actual removal of the mineral value in ore from the host rock or matrix (EPA, 2000). This study focuses on a site where extensive open pit mining has occurred. Surface mining with open pits has become the primary type of mining operation for most of the major metallic ores in the U.S., and these operations can affect groundwater, surface water, and associated sediments in several ways. Dissolved pollutants at a mine site are primarily heavy metals but may include sulfates, nitrates, and radionuclides (EPA, 2000). The primary constituents of concern for the study area for this report involve metals and radionuclides.

Remediation efforts at abandoned mine sites involve identifying sites and aspects of particular mining operations that have caused, or could result in, damage to the environment and loss of land use values (Robertson, 1996). The first step in the mine remediation process is to characterize the site, which involves assessing the potential environmental effects of the existing conditions. The following section presents an overview of environmental monitoring related to the project objectives.

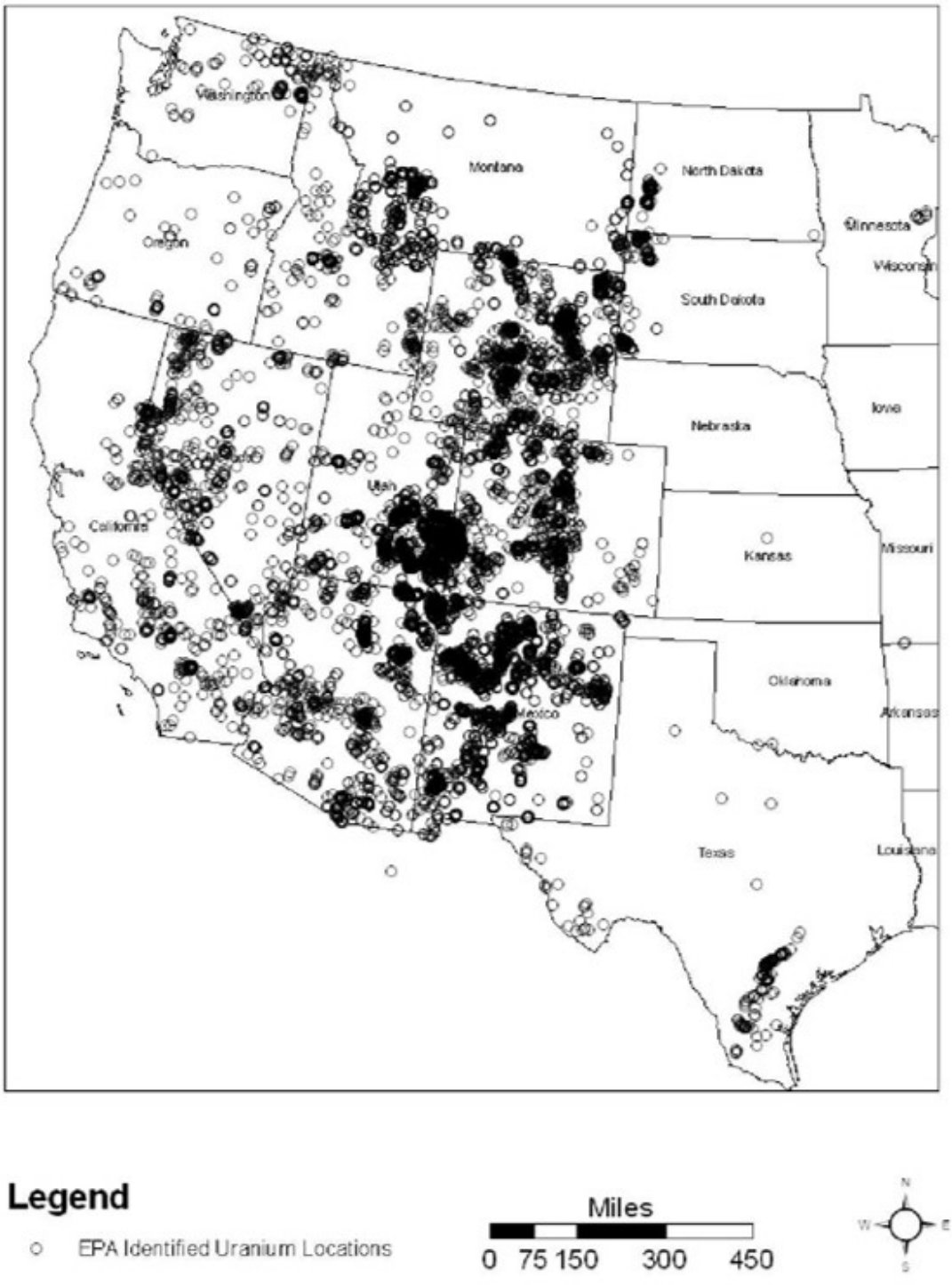

Figure 2 Western Uranium Locations From EPA Uranium Location Database (EPA, 2006)

2.2 ENVIRONMENTAL MONITORING

2.2.1 Overview

Environmental monitoring studies may be divided into several categories. For this study, environmental monitoring refers to data that are collected to characterize ambient concentrations in soil media. The specific data of interest is soil concentrations of target analytes including arsenic, uranium, and radium-226. These specific contaminants have been identified as the main risk drivers at the study area of interest, and their widespread transport has been exacerbated from anthropogenic activities, specifically the strip mining that occurred at the study area in the past. The data collected as part of this study involved innovative double sampling techniques that provide a rapid, accurate, and cost-effective method compared with slower and more expensive conventional soil sampling techniques. The data collected at the site provides information on these target analytes for estimating the spatial extent of soil contamination.

For an environmental study to be considered scientifically defensible and reputable, the monitoring program should follow established statistical methods that are both valid and reproducible, referred to as *statistics of environmental monitoring*. The application of statistics to environmental pollution monitoring studies requires a knowledge of statistical analysis methods particularly well suited to pollution data (Gilbert, 1987). The tools presented in this report consist of hot spot location techniques to quantify the extent of spatial contamination of the contaminants of concern at the study area. This section presents a literature review of the environmental pollution monitoring methods used to characterize the study area.

2.2.2 Contaminants of Concern

A risk-based standard for a contaminant is a specified fixed concentration value that is assumed to be known with certainty (EPA, 1996). This standard is usually established on the basis of human health or ecological risk assessments. A risk-based approach has been used at the Riley Pass site to date (USFS 2007, 2010). As described in Section 3.1.1, 40 Code of Federal Regulations (CFR) 192 sets concentration limits for cleanup of radium-226 and thorium at inactive uranium processing sites designated for remedial action; however, these standards are applicable only to Uranium Mill Tailings Radiation Control Act (UMTRCA) sites that are exempt from the Comprehensive Environmental Response, Compensation, and Liability Act (CERCLA). Two previous action memorandums established by the USFS (USFS 2007, 2010) specified removal cleanup criteria for soil using the risk-based approach. The EPA's target risk criterion for lifetime cancer risk is 1×10^{-4} to 1×10^{-6} carcinogenic range based on the reasonable maximum exposure for an individual (EPA 1997b).

Under EPA guidance, specifically Office of Solid Waste and Emergency Response (OSWER) 9355.7-04 (EPA 1995), a baseline risk assessment generally needs only to consider reasonably anticipated future land use; however, it may be valuable to evaluate risks associated with other land uses. A comprehensive risk assessment was performed by Portage Environmental Inc. (Portage) in 2006, and the results were presented in the *Final Human Health and Ecological Risk Assessment for the Riley Pass Uranium Mines in Harding County, South Dakota Revision 2* (Portage 2006). The Portage risk assessment is cited in Section 2.4 of Department of Energy (DOE) (2014) and in Section 3 of EPA (2008). The risk assessment was based on scientific and environmental data collected by Pioneer in 2002 and from

supplemental characterization work performed by Portage in 2004 (USFS 2006; Portage 2006). Re-examination of the risk based standards was performed by Tetra Tech in 2015 (Tetra Tech 2015) and soil cleanup standards for the project site were identified for a number of contaminants of potential concern (COPCs). The proposed cleanup levels for Riley Pass were evaluated for their potential risks (carcinogenic) and hazards (noncarcinogenic) to receptors who may be present at the site. The proposed soil cleanup values for the Riley Pass site are as follows:

- Arsenic: 142 milligrams per kilogram (mg/kg)
- Molybdenum: 2,775 mg/kg
- Uranium (U)-238: 42.8 pCi/g
- U-234: 44.6 pCi/g
- U-235: 2.03 pCi/g
- Radium (Ra)-226: 30.0 pCi/g
- Thorium (Th)-230: 39.8 pCi/g

Exposure to uranium and radium and other contaminants in abandoned mine waste can increase a person's risk of cancer. The exposures associated with the highest risks at the Riley Pass site are ingestion of arsenic in soil and external radiation from radium-226. The combination of arsenic and radium-226 produces very high cancer risks to potential on-site residents (EPA 2008). The costs associated with screening multiple contaminants during the removal action and the verification sampling will be greatly reduced if only arsenic and radium-226 need to be measured. Therefore, Tetra Tech analyzed the possibility of solely estimating cleanup boundaries based on arsenic and radium-226 and assessing the potential removal of the other COPCs. It was concluded in Tetra Tech (2015) that removal actions in reducing the arsenic and radium-226 concentrations in soil below the established soil cleanup levels will also reduce the other COPCs identified above. However, uranium is also evaluated for this study.

2.2.3 Hot Spot Location Statistical Techniques

Hot spot location techniques involve systematic sampling from a grid of sampling points arranged in a particular pattern. A "hot spot" refers to any sample that exceeds a cleanup standard for a specified contaminant of concern. Using statistical hot spot location techniques outlined in Gilbert (1987) and EPA (1989), the required sampling grid size can be calculated that corresponds to a probability of identifying a hot spot of a given size and shape. In practice, environmental monitoring programs are seldom conducted solely to accurately estimate the population mean; instead, a sampling design to delineate the spatial characterization of a particular contaminant is often the primary objective. Any samples that contain less than the site-specific cleanup criterion (< 142 mg/kg for arsenic; < 30 picoCuries per gram [pCi/g] for Ra-226) are assumed to be "clean," and no action is required. Furthermore, any surface soils exceeding the cleanup criterion (≥ 142 mg/kg for arsenic; ≥ 30 pCi/g for Ra-226) are considered contaminated and need to be excavated and isolated.

The grid spacing required for finding a specified hot spot of a pre-defined size and shape with a specified level of certainty can be established using the following procedure:

1. Specify L, the length of the semi-major of the smallest hot spot to detect. L is one-half the length of the long axis of the ellipse.

2. Specify the expected shape (S) of the elliptical target (S = 1 for a circle), where S is the length of the short axis of the ellipse divided by the length of the long axis of the ellipse. The target hot spot is assumed.
3. Specify an acceptable probability, referred to as "consumer's risk" (β) of not finding the hot spot.
4. Refer to Figure 3 below. The curves provided in this figure show the relationship between β and L/G, where G is the required grid spacing.

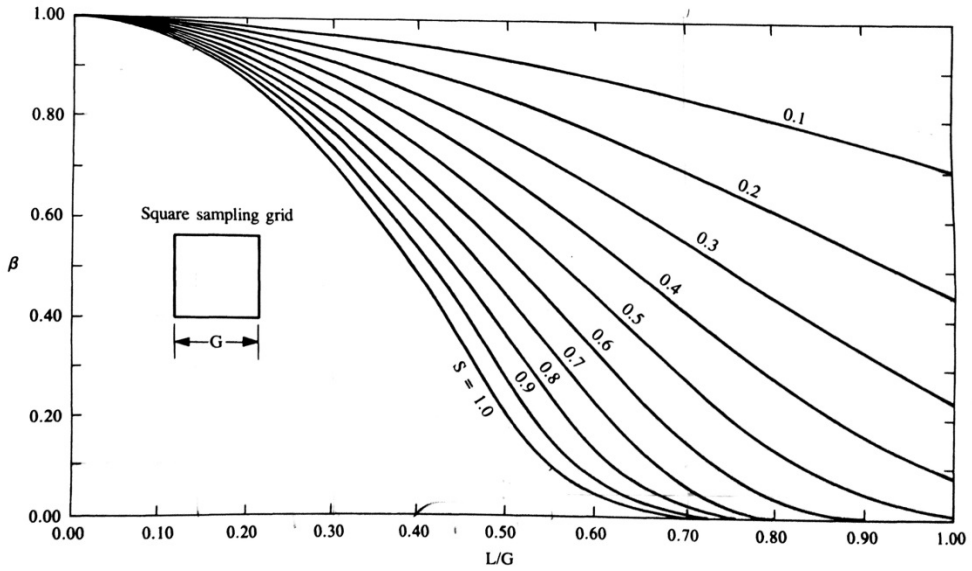

Figure 3 Curve's relating L/G to consumer's risk (Gilbert, 1987)

2.2.4 Double Sampling Statistical Techniques

Frequently, two or more techniques may be available for measuring the amount of contaminant in an environmental sample (Gilbert, 1987). Double sampling involves collection of a large set of samples by an inexpensive and less expensive rapid analytical method ("fallible" method) and a second smaller set of samples collected and analyzed by a more expensive and accurate method ("infallible") of analysis. The required grid spacing for sampling the surface soils must be relatively small to create a high probability that smaller hot spots will be found; given the size of the site, the cost of sampling and analysis can be high. The following condition must be met to assess whether double sampling is economically advantageous compared with simple random sampling (Gilbert, 1987):

$$R = \frac{C_A}{C_I} > \frac{\left(1 + \sqrt{1 - r^2}\right)^2}{r^2}$$

Where:

R = cost ratio

C_A = cost of accurate ("infallible") method

C_I = cost of more inaccurate ("fallible") method

r = correlation coefficient between two methods

Double sampling will be cost effective if the linear correlation between measurements obtained by the two techniques is sufficiently near unity and if the fallible method is substantially less costly than the more accurate method (in other words, has a higher cost ratio). The optimum number of infallible and fallible samples that should be collected can be calculated by the methods outlined in Gilbert (1987); however, the optimum number of samples determined by the double sampling procedures were not collected since both techniques used in this study rely on scientifically accepted procedures. For this particular study, the number of fallible and infallible samples required for each method is selected based on the specific sampling procedure for those methods. Since the optimum sample size requirements for the double sampling method are not achieved, it is not guaranteed that the linear regression double sampling approach will yield a more precise, on average, estimate of the mean than would be achieved by simple random sampling. Minimizing the variance of the estimated mean is not the primary objective of this study, however. The primary objective is to characterize the spatial extent of arsenic and radium-226 contamination using a reliable and cost-effective sampling approach. The equation presented above can be used to qualitatively assess whether double sampling should be used, based on cost and estimation accuracy, compared with simple random sampling.

2.2.4.1 XRF Field Survey

X-ray fluorescence (XRF) field surveys are widely used in the field of environmental engineering as a non-destructive, cost–effective, and rapid tool for screening soils or characterizing hazardous waste sites or sites contaminated with mine waste. The XRF is considered the “fallible” sampling technique because it is less expensive and provides instantaneous results when compared with the “infallible” sampling technique, consisting of conventional soil sampling and subsequent laboratory analysis. The XRF measurements taken directly from on-site surface soils are referred to as *in situ* XRF measurements. The XRF uses an X-ray tube to irradiate soil samples. The source X-rays excite electrons in the surface soil sample (EPA, 2007), dislodging electrons from atomic shells and creating vacancies. The vacancies are filled by the ray spectra as they cascade down to fill the inner shell vacancies. This process allows the XRF instrument to identify elements present based on the unique spectra emitted and to estimate metal concentrations in soil based on emitted flux. The XRF collects data from 26 analytes; however, the contaminant of concern for this particular site is arsenic. EPA method 6200 also specifies that one of every 20 XRF samples be collected and submitted for laboratory analysis. The samples submitted to the laboratory are referred to as *confirmation samples*. A site-specific linear correlation can then be made between the in situ XRF arsenic measurements and the arsenic concentration reported in the confirmation soil samples. The data should be log-transformed in cases where the data spread over more than one order of magnitude. The data can be used as a screening-level tool if the correlation coefficient is greater than 0.7. If the correlation coefficient is greater than 0.8, the correlation can be used to estimate that specific contaminant at a definitive level. Stringent quality assurance and quality control (QA/QC) procedures are followed as outlined in EPA Method 6200.

2.2.4.2 Gamma Radiation Survey

Using gamma radiation to estimate radionuclides is a common approach at sites contaminated with windblown uranium tailings (such as former uranium mills) and at abandoned uranium mines. The success of this approach depends on whether radionuclides of interest have gamma emissions, potential contamination is located on the ground surface and, most importantly, acquiring regulatory approval of the technique (Albequist, 2000). All soils and rock exhibit differing levels of radioactivity, depending on varying levels of naturally occurring potassium, uranium, thorium, and radium. On open ground, about two-thirds of the measured gamma radiation dose comes from radionuclides contained in the top 15 centimeters (cm) of soil (NRC, 1994). The objective of the continuous gamma radiation survey is to characterize the spatial distribution of gamma radiation emanating from surface soils at the site. Using soil correlation methods, the gamma data can then be used to predict the radionuclide concentrations in surface soils. A strong correlation must exist between the two parameters for the gamma radiation survey to be an effective tool to estimate radium-226 concentrations in soil. Correlation sampling is performed in accordance with the methods outlined in Johnson et al. (2006) and Whicker et al. (2008). After a gamma radiation survey is completed, field personnel select 10-meter (m) x 10-m (100 square meters, or m^2) correlation plot locations. The plot locations are selected to represent the range of gamma radiation at the site and in areas where homogeneity in the gamma field was observed. Composite soil samples from each plot are then submitted for laboratory analysis of radium-226 by gamma spectrometry using EPA Method E910.1. Gamma exposure rate data were collected within the boundary of each correlation plot using the scanning systems in the gamma radiation survey. Stringent QA/QC protocols are followed for all gamma survey projects relying on guidance from the Multi-Agency Radiation Survey Site Investigation Manual (MARSSIM) (NRC, 2000).

2.2.5 Geospatial Interpolation

The 2007 Action Memorandum (USFS, 2007) specifies that the mine areas are to be divided into appropriate sized grids and a block averaging technique applied to the post-reclamation data after the site has been reclaimed. Geospatial interpolation involving the use of geostatistical and deterministic methods were selected to meet the block averaging objective. Geostatistical methods are a powerful tool for mapping spatial data and providing interpolation between existing data points that have been collected (EPA, 1989). Geostatistical methods are commonly used in geographic, geological, and environmental sciences, as outlined in Journel and Huijbregts (1978), David (1977), and Verly et al. (1984). Two geostatistical methods were utilized for this study: kriging and the inverse distance weighted (IDW) method. Kriging is used to interpolate the denser gamma radiation point data, and IDW is used to interpolate between the more scattered XRF point data. There are two types of geospatial interpolation methods that were evaluated for this investigation: (1) deterministic and (2) geostatistical. These methods are described in more detail below.

2.2.5.1 Deterministic Methods

The IDW and radial basis function (RBF)methods are local deterministic interpolation techniques that calculate predictions from measured points within specified neighborhoods, which are smaller spatial areas within the larger study area. An interpolation technique that predicts a value identical to the measured value at a sampled location is known as an exact interpolator. The IDW and RBF are both exact interpolators. The IDW method creates surfaces based on the extent of similarity, and the RBF creates surfaces using a degree of smoothing (ESRI 2015). Deterministic interpolation techniques create surfaces from measured points, based on either the extent of similarity (inverse distance weighted) or

the degree of smoothing (radial basis functions). For this study, the IDW and RBF method were both evaluated.

2.2.5.2 Geostatistical Methods

Geostatistical interpolation techniques (kriging) use the statistical properties of the measured points. Geostatistical techniques quantify the spatial autocorrelation among measured points and account for the spatial configuration of the sample points around the prediction location (ESRI 2015). Geostatistical interpolation techniques use statistics for more advanced prediction surface modeling that also includes errors of predictions. Kriging is a geostatistical method that quantifies the spatial structure of the data and produces predictions. Kriging uses variography, fitting a spatial-dependence model to the data. Geostatistical Analyst provides many tools to help determine which parameters to use, and defaults are provided so that a surface can be created quickly (ESRI 2015). The types of kriging method used for this study included simple and ordinary. Figure 4 presents a screenshot from the Geostatistical Analyst program in ArcGIS 10.0 used for this study.

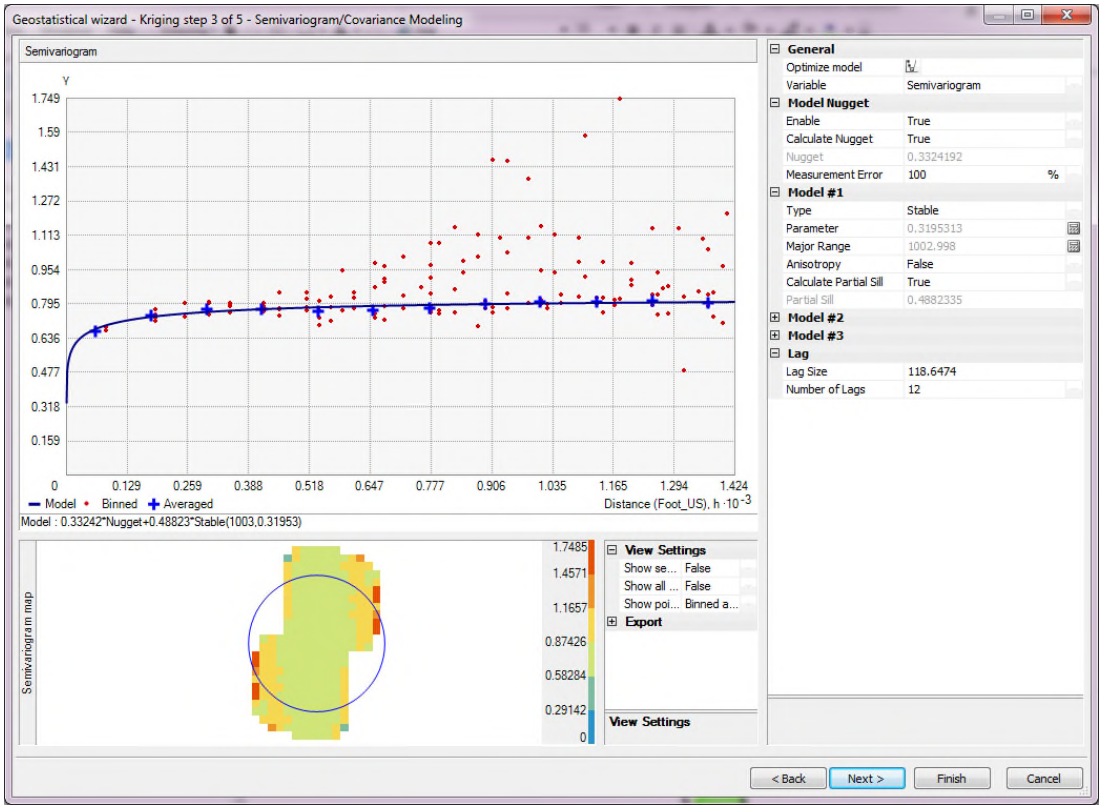

Figure 4 Screenshot of Semivariogram Modeling from Geostatistical Analyst Tool in ArcGIS 10.0

2.3 EROSION AND SEDIMENTATION

2.3.1 Overview

Erosion and sedimentation refer to the motion of solid particles, referred to as sediment (Julien, 2010). Sedimentation embodies the processes of erosion, entrainment, transportation, and the compaction of sediment (Vanoni, 1975). These natural processes have been active throughout geological times and have shaped the present landscape of the world. These processed and the deposition of fluvial sediment are complex, and the detachment of particles occurs through the kinetic energy of raindrop impact, or by forces generated by flowing water (Vanoni, 1975). In the past century, a distinction between natural geological erosion and human-induced erosion was admitted (Vanoni, 1975). Human activities usually accelerate the processes of erosion, transport, and sedimentation (Julien, 2010). A variety of human activities disturb the land surface of the earth and thereby alter natural erosion rates (Toy et al., 1998), and in some cases the erosion rate can be 100 to 1,000 times greater than the geological erosion rate of 0.1 ton/acre-year [about 25 ton/km^2-year] (Julien, 2010). The baseline geological erosion rates can be even higher in areas where the natural geological erosion rate is characterized as in “rapid retreat”, as seen at the Riley Pass site (Stone et. Al., 2007), and mining can exacerbate these erosion rates further.

The distinction between natural erosion processes and those caused by human influences is often difficult (Goy, 2015). However, this study evaluates a specific site where the human-induced impacts of strip mining has been well documented and the environmental impacts have been studied in detail. Mining operations may introduce large volumes of sediment directly into streams. Mine dumps and spoil banks, which are left ungraded and unvegetated, often continue to erode by natural rainfall for many years after mining operations have ceased (Julien, 2010; Vanoni, 1975). This study looks at the effects of strip mining as a potential major accelerator to the processes of erosion and sediment transport for particular study area at a localized level. The following sections present an overview of erosion processes specific to the study area and predictive methods for gross erosion soil loss rates and sediment delivery.

2.3.2 Erosion Processes

There are several erosion processes, including splash, sheet, rill, gully, and stream bank erosion. Splash erosion starts when raindrop impact on the ground surface detaches particles (Julien, 2002). The kinetic energy released by the impact of a raindrop on the ground is sufficiently large to break bonds between soil particles, and the characteristics of raindrop splash depend on raindrop size and sheet-flow depth (Julien, 2002). Upland erosion by water can be classified by sheet erosion and rill erosion (Julien, 2002). After the particles are detached from splash erosion, they are transported to rills by thin overland flow. Rill erosion is an erosion process that occurs when water from the sheet erosion combines to form small concentrated channels (Fortuin, 2006). Examples of splash erosion, sheet erosion, and rill erosion at a mine-impacted area at a localized region of Riley Pass is presented in Figure 5. Figure 6 shows the erosion processes affecting a designed repository at Riley Pass which had only been in place for less than 1 year.

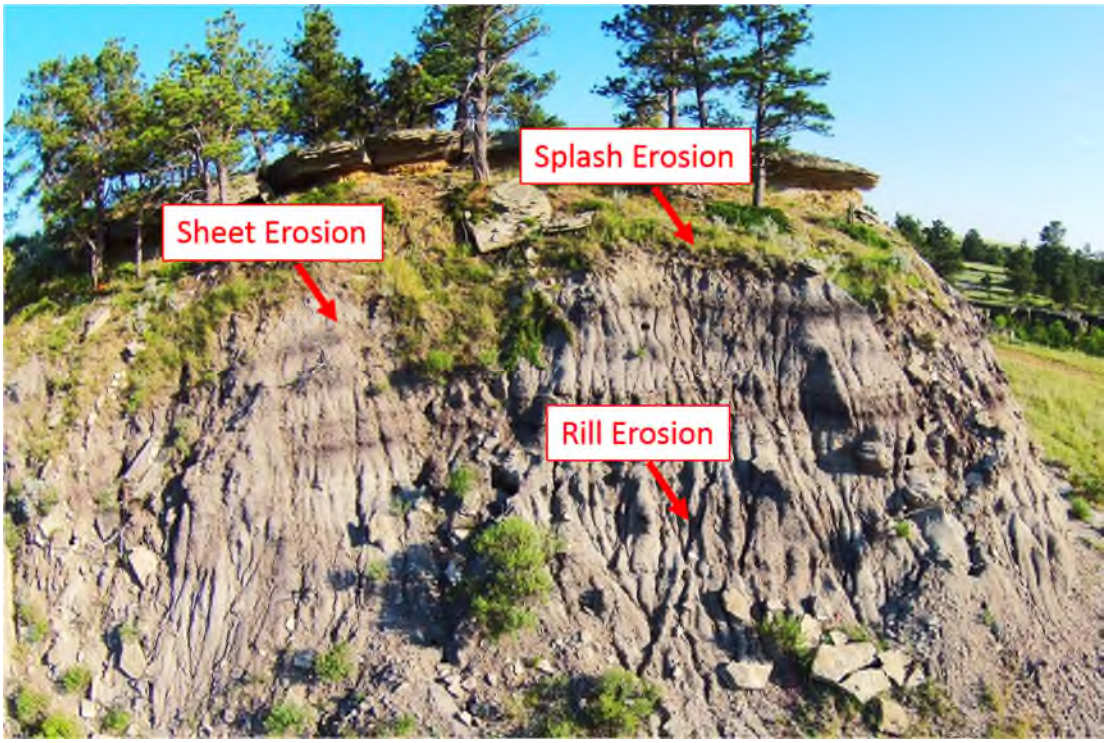

Figure 5 Localized Erosion Processes at a Mine Impacted Bluff at Riley Pass

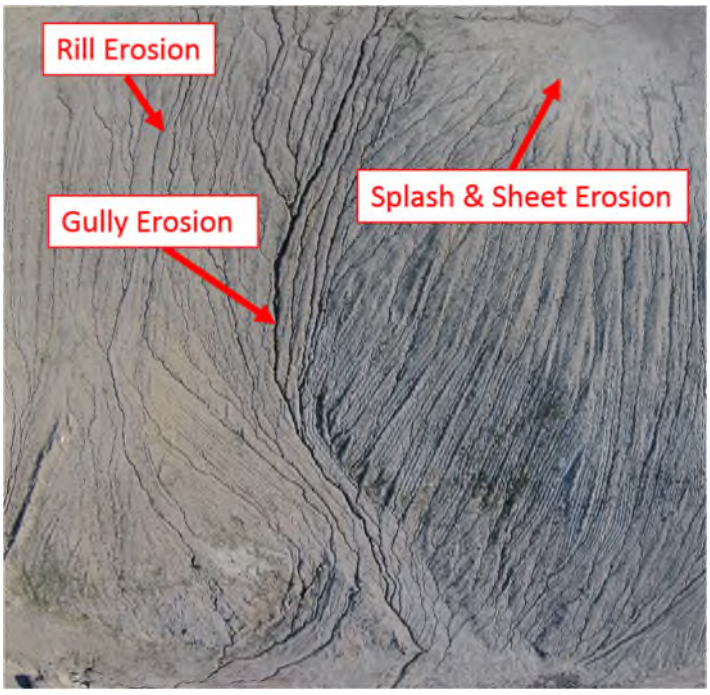

Figure 6 Localized Erosion Processes at a Mine Impacted Bluff at Riley Pass

The concentration of runoff under some circumstances encourages the formation of gullies (Vanoni, 1975). When water in rills concentrate to form larger channels, it results in gully erosion (Fortuin, 2006). At Riley Pass, severe climatic events coupled with improper reclamation from past mining practices have led to development of gulley systems, further exacerbating the delivery of contaminated sediment into downstream river systems. An example of a large gulley system at Riley Pass is shown in Figure 7, where the gulley formation is tens of meters deep. The primary concern at Riley Pass is development of extensive gully networks and the subsequent transport and deposition of contaminated sediment on the tailings piles and materials exiting the watershed, further deteriorating water quality in the surrounding environment.

Figure 7 Example of Gully Erosion on Eastern Side of Bluff B at Riley Pass

2.3.3 Gross Erosion Soil Loss

The need for factual, quantitative information to calculate soil erosion rates under a variety of climatic, physiographic, land use, and soil management situations led to the establishment of small research test plots as early as 1917 in the U.S (Vanoni, 1975). General relationships were developed from data of plot studies of sheet erosion that could be used by soil-water resource planners to predict the long-term erosion rate for a given variety of land-use programs (Vanoni, 1975). In 1947, the empirical Musgrave equation was developed that incorporated a rainfall parameter. Several erosion models have been developed in the past few decades.

One of the major innovations in soil and water conservation during the past century was the development of the Universal Soil Loss Equation (USLE). The USLE is a powerful tool that has been used by soil conservationists for on-farm planning of soil conservation practices, inventorying and assessing the regional and national impacts of erosion, and developing and implementing public policy related to soil conservation (Renard et al., 1991). The USLE was developed by W.H. Wischmeier, D. D. Smith, and others with the USDA, Agricultural Research Service (ARS), Soil Conservation Service (SCS), and Purdue University in the late 1950s (Renard et al., 1991). The original USLE model is limited in that it is effective only at predicting soil loss for mild slopes sensitive to rill and inter-rill erosion (Van Remortel et al., 2001). The USLE was introduced at a series of regional workshops on soil-loss prediction in 1959 through 1962 by the USDA (Renard et al., 1997). Finally, USLE was presented in Agriculture Handbook No. 282 (Wischmeier and Smith, 1965). Widespread acceptance of USLE took time but came progressively as more regions and groups began using the equation.

Incorporating many improvements from the original model, an updated USLE was presented in Agriculture Handbook No. 537 (Wischmeier and Smith, 1978). Further successive efforts to improve the USLE has been made by researchers in the last 3 decades (Goy, 2015), resulting in numerous models including: the Modified Universal Soil Loss Equation (MUSLE) developed by Williams in 1975, the Areal Nonpoint Source Watershed Environmental Simulation [ANSWERS] (Beasley et al., 1980), the Guelph Model (Rudra et al., 1986), the Unit Stream Power- based Erosion Deposition [USPED] (Mitasova et al., 1996), and the Revised Universal Soil Loss Equation [RUSLE] (Renard et al., 1997).

The RUSLE is an empirical erosion model designed to predict the long-time average annual soil loss (A) carried by runoff from specific field slopes in specified cropping and management systems as well as from rangeland areas (Renard et al., 1997). Widespread use of this model has substantiated the usefulness and validity for these purposes, but it is also applicable to nonagricultural construction sites, mined lands, and reclaimed lands (Renard et al., 1997; Toy et al., 1998).

Both the USLE and the RUSLE equation can be defined as follows (USDA 1997):

Equation 1 $$A = R \cdot K \cdot L \cdot S \cdot C \cdot P$$

Where

A = computed spatial average soil loss and temporal average soil loss per unit of area, expressed in the units for K and for the selected period, R.
R = rainfall-runoff erosivity factor
K = soil Erodibility factor
L = slope length factor
S = slope steepness factor
C = cover management factor
P = support practice factor

The use of GIS in environmental engineering has seen an unprecedented growth in the recent past. GIS software captures geographic data for manipulation, viewing, and analysis (ESO, 2015). The increased popularity of GIS technology and availability of Digital Elevation Models (DEM) has led to wide recognition of using DEMs in studies of surface processes including prediction of the spatial extent of gross soil loss rates. Additionally, the automated generation of drainage networks has become increasingly popular with powerful analytical functions in GIS and with the increased availability of DEMs (Wang et al., 1997). The RUSLE model has advantages because the data requirements are not too complex or unattainable, it is relatively easy to understand, and it is compatible with GIS (Millward et al., 1999). Numerous studies integrating the RUSLE model combined with GIS techniques to analyze the spatial extent of gross soil loss rates have been successfully performed in the past two decades, including but not limited to Millward et al. (1999), Boggs et al. (2001), Hua et al. (2006), Kim (2006), Zeilhofer (2008), and Goy (2015).

The variability in natural site conditions combined with significant differences in the quantities and characteristics of exposed materials at mines preclude any generalization of the quantities and characteristics of sediment loadings (EPA, 2000). The erosion rate for a given site results from the combination of many physical and management factors. This study presents the development of a spatially based RUSLE model utilizing GIS techniques to model gross soil loss rates at the Riley Pass site. The linking of on-site rates of erosion and soil loss within a drainage basin to the sediment yield at the basin outlet is presented in Section 2.3.4.

2.3.4 Sediment Delivery

The previous subsection presented historical, theoretical, and practical approaches to the estimation of mean annual gross erosion from a watershed. It is well known that only a fraction of the sediment eroded within a drainage basin will find its way to the basin outlet and be represented in the sediment yield (Walling, 1983), so for example, the rate at which sediment is carried by natural streams is much less than the gross erosion on its upstream watershed (Julien, 2010). The relative magnitude of this loss tends to increase with increasing basin size (Walling, 1983). The term *sediment yield* is defined by Vanoni (1975) as the total sediment outflow from a watershed or drainage basin. Sediment yield rates are estimated using average basin characteristics such as basin size, drainage density, mean slope, mean land cover, and mean soil type (Anton, 2001). Sediment delivery to river channels is probably the most problematic off-site consequence of soil erosion (Anton, 2001). These off-site problems can become increasingly more important if the sediment being delivered is contaminated with environmental pollutants such as heavy metals and radionuclides, as is the case with the particular study area of interest.

The term *sediment delivery* has been widely used to represent the resultant of various processes involved between on-site erosion and downstream sediment yield (Walling, 1983). The concept of *sediment delivery ratio* can be defined as the ratio of sediment delivered at the catchment outlet (t km^{-2} yr^{-1}) to the gross erosion within the basin (t km^{-2} yr^{-1}). If the transport capacity is insufficient to sustain transport of material between the source and the stream, then sediment is deposited. The sediment delivery ratio, SDR, was introduced to quantify these effects by Glymph (1954), Maner (1958), and Roehl (1962). The SDR is effectively an index of sediment transport efficiency (Hua et al., 2006). Vanoni (1975) defines the SDR as a measure of diminution of eroded sediments, by deposition from the point of erosion to any designated downstream location, and can also be expressed as a percentage of the on-site eroded material that reaches a given measuring point. The *SDR* is a dimensionless scalar that denotes the ratio of the sediment yield (Y) at a given stream cross-section to the gross erosion (A_T) from the watershed upstream of the measuring point (Julien, 2010) and is represented as:

Equation 2

$$SDR = \frac{Y}{A_T}$$

Walling (1983) stated that there is a major research need for linking on-site rates of erosion and soil loss within a drainage basin to the sediment yield at the basin outlet. Numerous studies have attempted to produce empirical prediction equations for the SDR with the intention of providing empirical predictive equations for this variable that can be used to provide a ready means of estimating sediment yield of a basin from estimates of gross erosion obtained from using established procedures such as the USLE (Wischmeier et al., 1958). The magnitude of sediment delivery ratio for a particular basin is influenced by a wide range of geomorphological and environmental factors, including the nature, extent, and location of sediment sources, topographic relief and slope characteristics, the drainage pattern and channel conditions, vegetation cover, and soil texture (Walling, 1983). The large range of complex phenomena that need to be considered in trying to quantify sediment delivery makes it no surprise that a number of methods are available to estimate this parameter.

Methods to estimate the SDR can be roughly grouped into three categories (Hua et al., 2006). The first category involves specific sites where sufficient data are available such as sediment yield and stream flow data, which allow for methods using sediment rating curve-flow duration or reservoir sedimentation to be used. This approach is not feasible for the study area of interest based on the lack

of these types of available stream flow data. The second category attempts to build models based on fundamental hydrologic and hydraulic processes. Despite the merit of physical description used in these models, the existing models are often not suited to basin-scale applications such as the study area of interest. The third category uses empirical relationships which relate SDR to morphological characteristics of the watershed, such as the catchment area (Hua et al., 2006). The uncertainties surrounding the wide range of sediment delivery ratios reported by individual studies, and the lack of a generally-applicable predictive technique, are paralleled by fundament problems associated with the concept of a simple relationship between gross erosion and sediment yield (Walling, 1983). Many of these assessments on the SDR have themselves been based on measured sediment yield with an estimate of gross erosion from established procedures and are therefore open to considerable uncertainty from the reliability of these procedures themselves. Additionally, the problems with the idea of using a simple SDR relationship relates in particular to the temporal and spatial lumping inherent in the concept and to the its blackbox concept (Walling, 1983). These are important factors to consider in estimating sediment yield based on a set SDR and estimated gross erosion from a procedure like USLE or RUSLE. The third category described above attempts to quantify the linkage between source-area erosion and sediment yield by using a simplified empirical relationship between SDR and watershed area, which is commonly represented using the following SDR-area power function (Roehl, 1962):

$$SDR = \alpha A^{\beta}$$

Where A is the watershed area (in km^2), and α and β are empirical parameters. Statistical regressions based sediment measurements show that the exponent β is in the range -0.01 to-0.25 (Walling, 1983), indicating a decrease in SDR with an increase in watershed area. Three primary SDR equations are used in this study: Boyce (1975), Vanoni (1975), and SCS (1979).

Boyce (1975) established a relationship between sediment delivery ratio and drainage area by compiling and analyzing sediment yield observation from five areas in continental US. Equation 1 presents the power function:

Equation 3 (Boyce 1975) $SDR = 0.41A^{-0.3}\ (A\ in\ km^2)$

The USDA SCS (1979) developed a SDR model based on data from the Blackland Prairie, Texas. Equation 3 presents the power function developed by SCS (1979):

Equation 4 (USDA-SCS 1979) $SDR = 0.51A^{-0.11}\ (A\ in\ mi^2)$

Vanoni (1975) developed data from 300 watersheds throughout the world to develop an equation by the power function. This equation is considered a more generalized one to estimate the SDR (Kim, 2006). Equation 3 presents the power function developed by Vanoni (1975):

Equation 5 (Vanoni 1975) $SDR = 0.42A^{-0.125}\ (A\ in\ mi^2)$

Sediment yield, Y, is the total sediment outflow from a drainage basin, or watershed, over a specified period of time (Julien and Kane, 2007). The sediment yield from Julien (2010) can be written as follows:

Equation 4 $$Y = A_T S_{DR}$$

Specific degradation refers to the ratio of the sediment yield, Y, divided by the drainage area, A, as follows:

Equation 5 $$SD = \frac{Y}{A}$$

The following section presents the methodology for development of the soil contaminant mapping, stream network delineation, and soil erosion modeling.

3.0 METHODOLOGY

3.1 SOIL CONTAMINANT MAPPING

3.1.1 Overview

An objective of this study is estimate the amount of contamination being transported off the site based on the available information. It is important to understand the magnitude and spatial extent of arsenic, uranium, and radium-226 concentrations present within surface soil of the study area to provide accurate estimates of the amount of contaminant being transported. This section presents the methods for data collection for the purposes of soil contaminant mapping.

3.1.2 Arsenic and Uranium Mapping

In situ XRF sampling as a double sampling method was determined to be cost effective compared with simple random sampling. Following EPA Method 6200, a strong correlation ($r > 0.8$) must be established between the in situ XRF measurements and the arsenic concentrations measured in the laboratory to be used as a definitive characterization tool. The in situ XRF measurements were collected throughout the site using a portable Niton XRF Xl3t spectrum analyzer. The field portable XRF procedures were performed in accordance with EPA Method 6200 – "*Field Portable X-ray Fluorescence Spectrometry for the Determination of Elemental Concentrations in Soil and Sediment*" (EPA, 2007). A total of 804 in situ XRF arsenic measurements (fallible samples) were collected from Bluff B and 69 confirmation samples (infallible samples) were collected from Bluff B and other areas and submitted for laboratory analysis. The confirmatory samples were selected from the lower, middle, and upper range of concentrations measured at the site. EPA Method 6020A was used for the analysis of total arsenic in the soil samples. The arsenic concentrations measured spanned four orders of magnitude; as such, these data were log-transformed to standardize the variance proportional to the magnitude of the measurement. Figure 8 shows the correlation between in situ XRF arsenic and laboratory-reported arsenic at the site. The correlation can be used as a definitive level characterization tool since the *r* is greater than 0.8 and inferential statistics indicate the confirmatory data are statistically equivalent at a 99 percent confidence level. A similar correlation was developed between the in situ XRF uranium and laboratory-reported uranium at the site; however, this model is not presented in this paper.

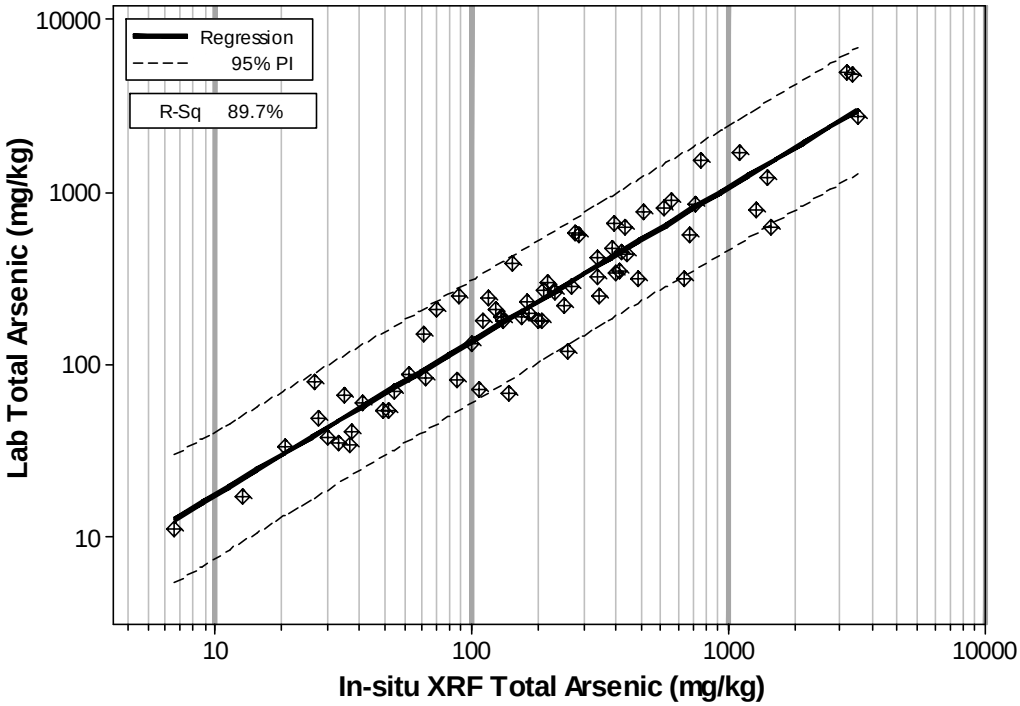

Figure 8 In situ XRF Arsenic Concentration vs. ICMP Lab Reported Arsenic Concentration

A strong correlation (r = 0.95) exists between the in situ XRF arsenic measurements and the laboratory-reported total arsenic concentrations. The following equation was used to convert the in situ XRF measurements to laboratory equivalent arsenic concentrations at the site:

$$Lab\ Arsenic\ = 10^{0.352+0.891 log_{10}(\text{XRF Arsenic})}$$

Where:

Lab arsenic = laboratory reported arsenic concentration in surface soil (mg/kg).

XRF Arsenic = XRF measured arsenic concentration in surface soil (mg/kg).

3.1.3 Radium-226

Field engineers used mobile backpack scanning systems consisting of 5-cm by 5-cm Ludlum 44-10 thallium laced sodium iodide (NaI(Tl)) scintillation detectors and Ludlum 2350-1 data loggers coupled with Wide Area Augmentation System (WAAS) enabled global positioning systems (GPS) connected to a field laptop. The gamma exposure rate data were transmitted once per second to a portable computer and logged using proprietary logging and mapping software (Tetra Tech, 2006). A detector height of 1 m above the ground surface is considered standard practice for this application (EPA, 1999, and OSD, 2012) and was used during this survey. All measurement data were automatically stored and processed with the measurement location information to be mapped and analyzed in real time. Real-time mapping allowed the field engineer to maintain position on pre-determined scan transect lines and to identify any problems that arose during the scanning efforts. NaI(Tl) detector systems exhibit energy-dependent response characteristics normalized to the cesium-137 0.662 megaelectronvolt (MeV) photon. The Ludlum 2350-1 data logger system employs a calibration factor to internally convert detector counts per

minute (cpm) to gamma exposure rate. The calculated exposure rate, directly proportional to the measured cpm, is transmitted by the data logger to the scanning system portable PC. The system does not retain a record of count rate, but count rate can be calculated using the instrument-specific calibration factor.

Gamma surveying as a double sampling method was determined to be cost effective compared with simple random sampling. Following methods in Johnson et al. (2006) and Whicker et al. (2008), a correlation between gamma radiation and Ra-226 concentration in soil was performed using 100 m^2 correlation plots throughout the site. A total of 22 soil correlation plots were surveyed for gamma radiation, and soil samples were collected and submitted to a laboratory for analysis of Ra-226 using gamma spectrometry (Method E.901.1). Since the gamma and radium concentrations measured spanned three orders of magnitude, the data were log-transformed to standardize the variance proportional to the magnitude of the measurement. Figure 9 shows the correlation between gamma exposure rate and Ra-226 concentration in soil at the site.

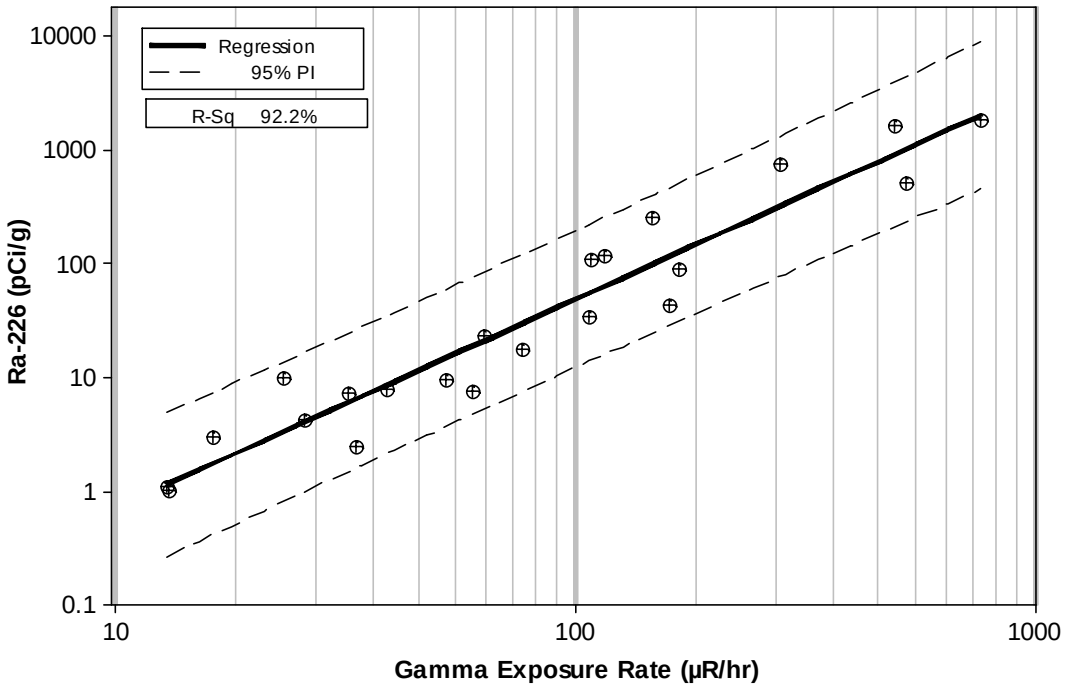

Figure 9 Gamma Exposure Rate vs. Soil Radium-226 Mass Activity Concentration

A strong correlation (r = 0.96) was established between gamma exposure rate and the Ra-226 concentration in soil. The following equation was used to convert the gamma radiation measurements collected at the site to laboratory equivalent Ra-226 soil concentrations:

$$\text{Lab Ra} - 226 = 10^{-1.979+1.835\ log_{10}(Gamma)}$$

Where:

Lab Ra-226 = laboratory equivalent soil radium-226 concentration (pCi/g).

Gamma = Gamma exposure rate measurement (µR/hr)

3.1.4 Geostatistical Methods

The environmental data sets were interpolated using deterministic (IDW and RBD) and geostatistical methods (simple and ordinary kriging). Continuous raster surface soil concentration grid maps for arsenic, uranium, and radium-226 were generated at the study area. A minimum of four scenarios were applied to each contaminant at the study area to determine the optimal geospatial interpolation method to be used for each contaminant raster surface. The analysis was performed using the Geostatistical Analyst tool in ArcGIS 10.1. The Geostatistical Analyst tool is a complete package for preprocessing data and for choosing an optimal interpolation strategy. The following interpolation methods were evaluated for each contaminant at each study area:

1. Scenario A: Inverse Distance Weighted (Deterministic method)
2. Scenario B: Radial Basis Function (Deterministic method)
3. Scenario C: Simple Kriging (Geostatisical method)
4. Scenario D: Ordinary Kriging (Geostatisical method)

The analysis involved a series of steps to evaluate the concentrations in soil at each study area using the interpolation methods described above and collecting output information that is provided by the program. In addition to evaluating the output parameters, a validation analysis was performed to determine how well the predicted concentrations matched the measured XRF or gamma converted concentrations. The most superior interpolation model was selected by analyzing the slope and correlation coefficient (R) of the best fit line of scatter plot of predicted vs. measured data points. An optimal model was selected for each contaminant (arsenic, uranium, and radium-226) at the study area after careful evaluation of the following criteria:

1. Evaluation of geostatistical parameters generated from the cross validation analysis, including the mean error, root mean square error (RMS), and the root mean square standardized error (RMSS).
2. Data validation to compare the predicted model results with the measured arsenic, uranium, and radium-226 in soil samples.

A combination of statistical diagnostics including cross validation and validation were used to determine which method best represents the measured data sets. Cross validation involves removal of one data location and then predicts the associated data point using the rest of the data locations. The purpose of cross validation is to gain useful information on the model parameters. The data sets used for validation were the measured in situ XRF measurements or gamma measurements collected in the field and then converted using the regression models. Examining the residuals is a key part of all statistical modeling diagnostics, since residuals indicate whether the chosen model is appropriate. The residuals between the predicted and measured soil concentrations were evaluated for model appropriateness. The final results of the soil contaminant mapping for the target analytes are presented in Section 4.0.

3.2 WATERSHED DELINEATION

3.2.1 Overview

The first step in any kind of hydrologic modeling involves delineating streams and watersheds and obtaining watershed properties such as area, slope, flow length, and stream network density. Historically, this step is done manually by using topographic maps. However, as a result of the advent of

GIS tools and DEM, these watershed properties can be extracted by automated procedures. The processing of DEM to delineate watersheds is referred to as terrain pre-processing. Arc Hydro tools is the method of choice for this project to process the DEM to delineate watershed, sub-watershed, stream network, and other characteristics.

3.2.2 Watershed Mapping

The first step of hydrologic modeling involves the delineation of streams and watersheds. This process is traditionally done manually using topographic and contour maps. With the availability of a high resolution DEM for the site, this process was handled using terrain preprocessing tools available in GIS. Five primary watersheds were identified using the GIS terrain preprocessing analysis tools; these basins were validated by comparing the results with a previous private study conducted by Tetra Tech in 2014. The watershed names were delineated by *North, East, Central, Southeast*, and *South*. These watersheds ranged in size between 16 acres (0.025 mi^2) to 94 acres (0.147 mi^2). Table 1 presents a summary of the watershed surface areas. Multiple smaller subbasins were identified for each watershed; however, since the watersheds are small (< 0.15 mi^2) the subbasins were merged into one individual subbasin representing each watershed. Similarly, the stream networks were delineated for each watershed. A map showing the stream network, watershed boundaries, and location of sediment ponds is provided on Figure 10. The primary sediment ponds to assess sediment yield include SP1, SP2, and SP3 that are shown on Figure 10.

Table 1 Summary of Watershed Areas

Watershed ID	Drainage	Basin Surface Area		
		mi^2	km^2	acres
North	Pete's Creek	0.067	0.17	43
East	Pete's Creek	0.113	0.29	72
Central	SP1	0.039	0.10	25
Southeast	SP2	0.025	0.07	16
South	SP3	0.147	0.38	94
Total		**0.391**	**1.01**	**250**

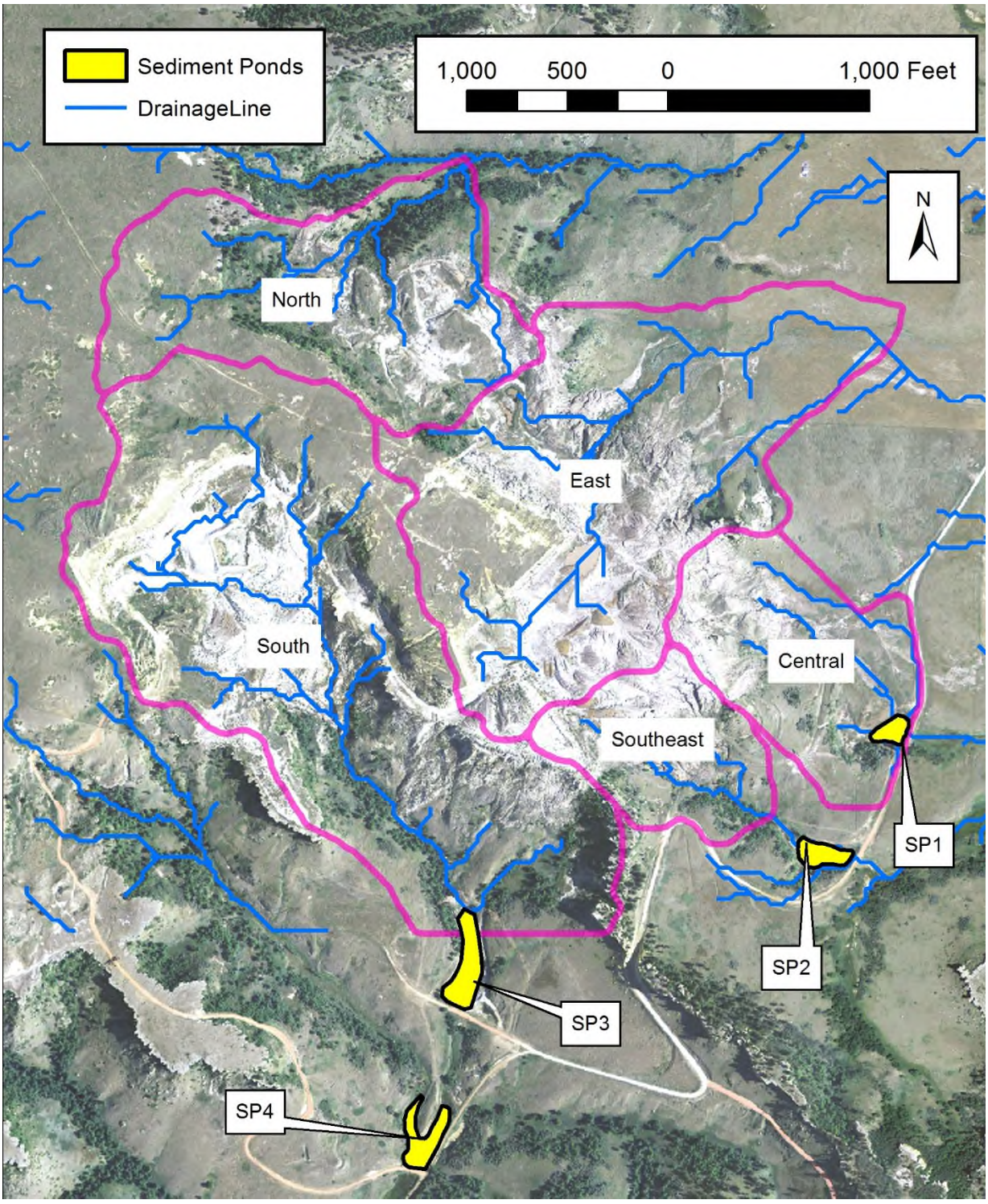

Figure 10 Stream Delineation and Watershed Map for Study Area

3.3 EROSION MAPPING

3.3.1 Overview

The RUSLE model parameters are introduced in Section 2.3.3. The RUSLE can be used to predict rainfall erosion in landscapes using GIS and is implemented by using spatially distributed soil, vegetation, topographical, and land use properties under a GIS environment. The RUSLE has a number of factors where data are needed. The following subsections discuss the data acquisition process for each of the RUSLE factors that was needed for development of an accurate GIS model. This study assumed that the conservation practice factor (P) was unity and is therefore not presented in this section.

3.3.2 Rainfall-runoff Erosivity, R Factor

The rainfall and runoff factor (R) of the USLE was derived from research from many data sources. Rills and sediment deposits observed after an unusually intense storm have sometimes led to the conclusion that significant erosion is associated with only a few severe storms and significant erosion is solely a function of peak intensities (Renard et al., 1997). However, Wischmeier (1962) evaluated more than 30 years of measurements in many states and concluded that only a few severe storms and significant erosion is not the a function of only peak intensities. The data from Wischmeier (1962) showed a rainfall factor used to estimate average annual soil loss must include the cumulative effects of the many moderate-sized storms as wells as effects of the occasional severe storms. Local values of the rainfall erosion index for this study were taken directly from an isoerodent map for South Dakota. The plotted lines shown in Figure 11 are called isoerodents because they connect points of equal rainfall erosivity (Renard et al., 1997). The isoerodent maps are based on more than 1,200 gauge locations in the western U.S. This parameter is highly affected by storm intensity, duration, and potential. The USDA created contours of the spatial variation of the R-factor throughout the continental U.S. An R value of 53 for the site was obtained from the isoerodent map of South Dakota shown in Figure 11.

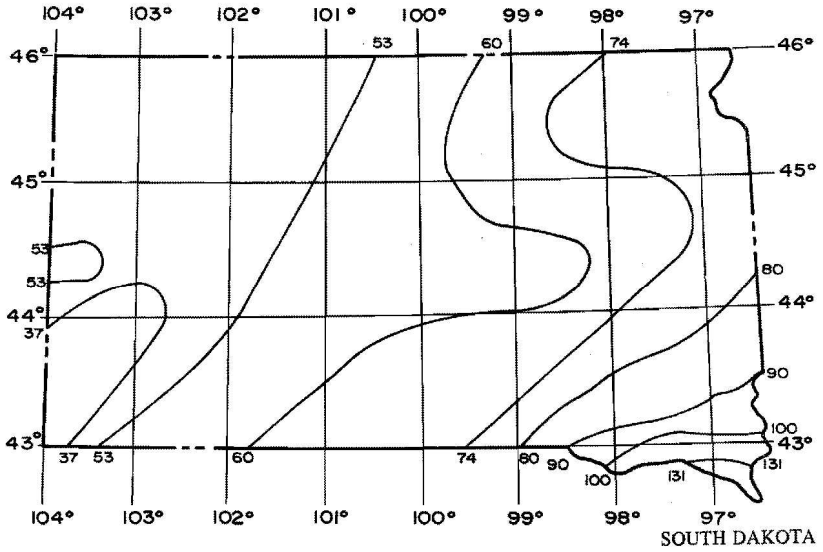

Figure 11 Isoerodent, R, Map of South Dakota

3.3.3 Soil Erodibility, K Factor

The soil erodibility factor (K factor) was presented in Equation 1 in Section 2.3.3. The K factor is the soil-loss rate per erosion index unit for a specified soil as measured on a standard plot, which is defined as a 72.6-foot (22.1 m) length of uniform 9 percent slope in continuous clean-tilled fallow (USDA, 1997). The K factor represents the (1) susceptibility of soil or surface material to erosion, (2) transportability of the sediment, and (3) amount and rate of runoff given in a particular rainfall input, as measured under a standard condition (Toy et al., 1998). The K factor indicates susceptibility of a soil to sheet and rill erosion by water. The K factor is one of the six factors used in the RUSLE to predict the average annual rate of soil loss by sheet and rill erosion in tons per acre per year.

The primary data acquisition method for the determination of the spatially based K factor for soil erosion modeling is soil surveys. Soil surveys are made to provide information about soils in a specific area. The data for the K factor for the two study areas were obtained from a custom soil resource report for Harding County, South Dakota, obtained from the Natural Resources Conservation Service (NRCS) web soil survey program for the areas of interest. A soil survey geographic (SSURGO) database file was downloaded for the project area. Soils data were available and were ground checked with aerial imagery, observations from site visits, and unmanned aerial vehicle (UAV) surveys. Overall, the soils report accurately reflect the ground conditions on the site, specifically with respect to the areas where mine dumps are currently located.. The K factor values for each soil type were provided in the soils report and ranged between 0.10 and 0.43. Table 2 presents the soil types found within the study area watersheds and the associated hydrologic soil groups, K factor, and percent of watershed.

Table 2 Soil Classification for Study Area, K Factor, and Percent of Watershed

Map Unit Symbol	Description	Hydrologic Soil Group	K Factor	Acres of Watershed	Percent of Watershed
BoD	Bullock-Cabbart Complex	D	0.43	0.64	< 1%
CcE	Cabbart Loam	D	0.10	10.2	4.1%
CoE	Cohagen Fine Sandy Loam	D	0.24	69.4	28%
CrF	Cohagen-Rock Outcrop Cabba	D	0.24	17.0	6.8%
Du	Mine Dumps	D	0.32	126	50%
PbB	Parchin-Bllock Fine Sandy	D	0.32	1.39	< 1%
RnB	Rhoades-Daglum Loams	C	0.32	25.9	10%

The soil map obtained from the NRCS web soil survey on-line service is provided in Figure 12. The soil classification map was used to generate a K Factor map for all of the watersheds. Figure 13 presents the spatial distribution of the K factor values used in the GIS application of the RUSLE model.

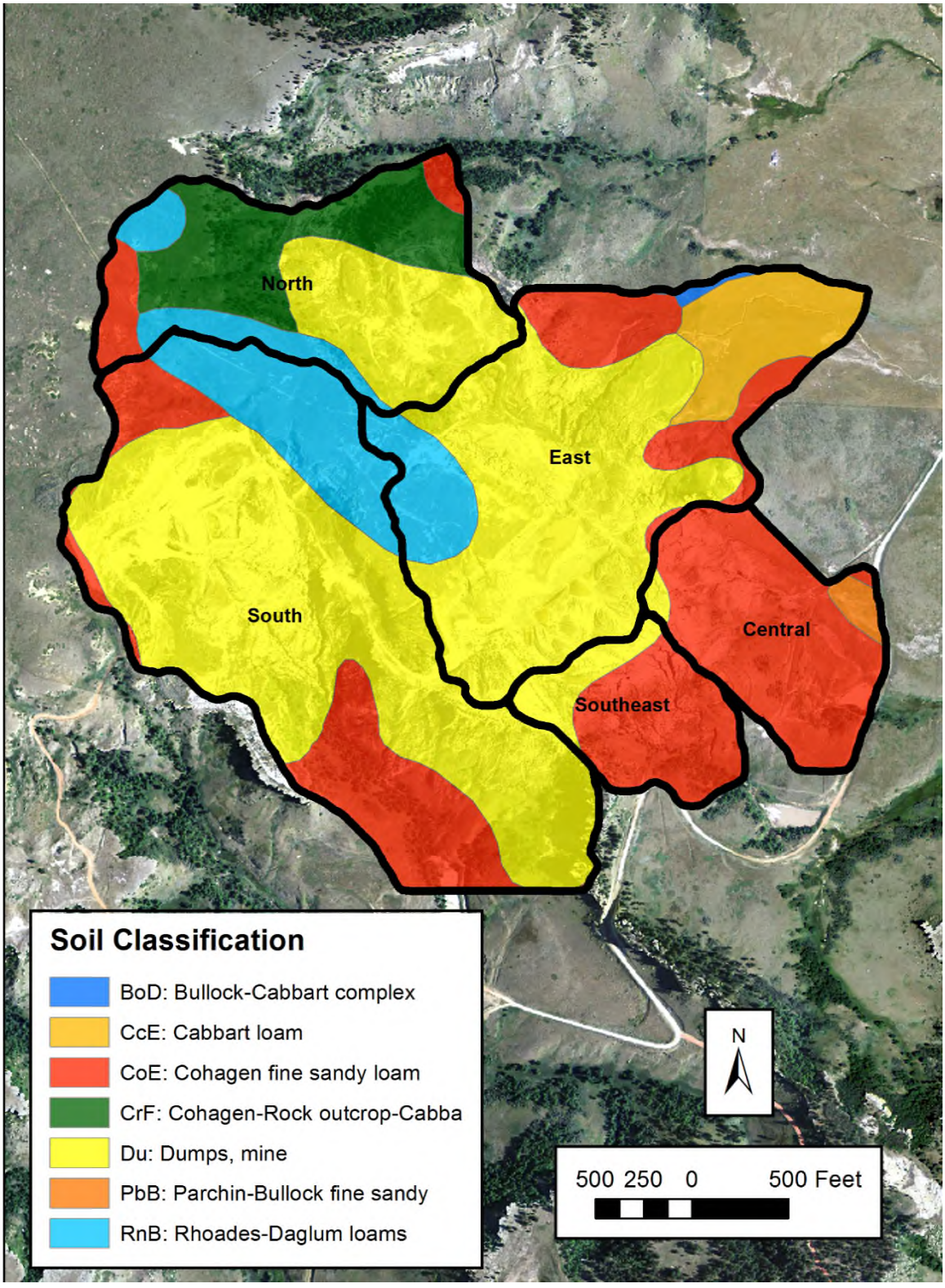

Figure 12 Soil Classification Map for Bluff B Watershed Areas

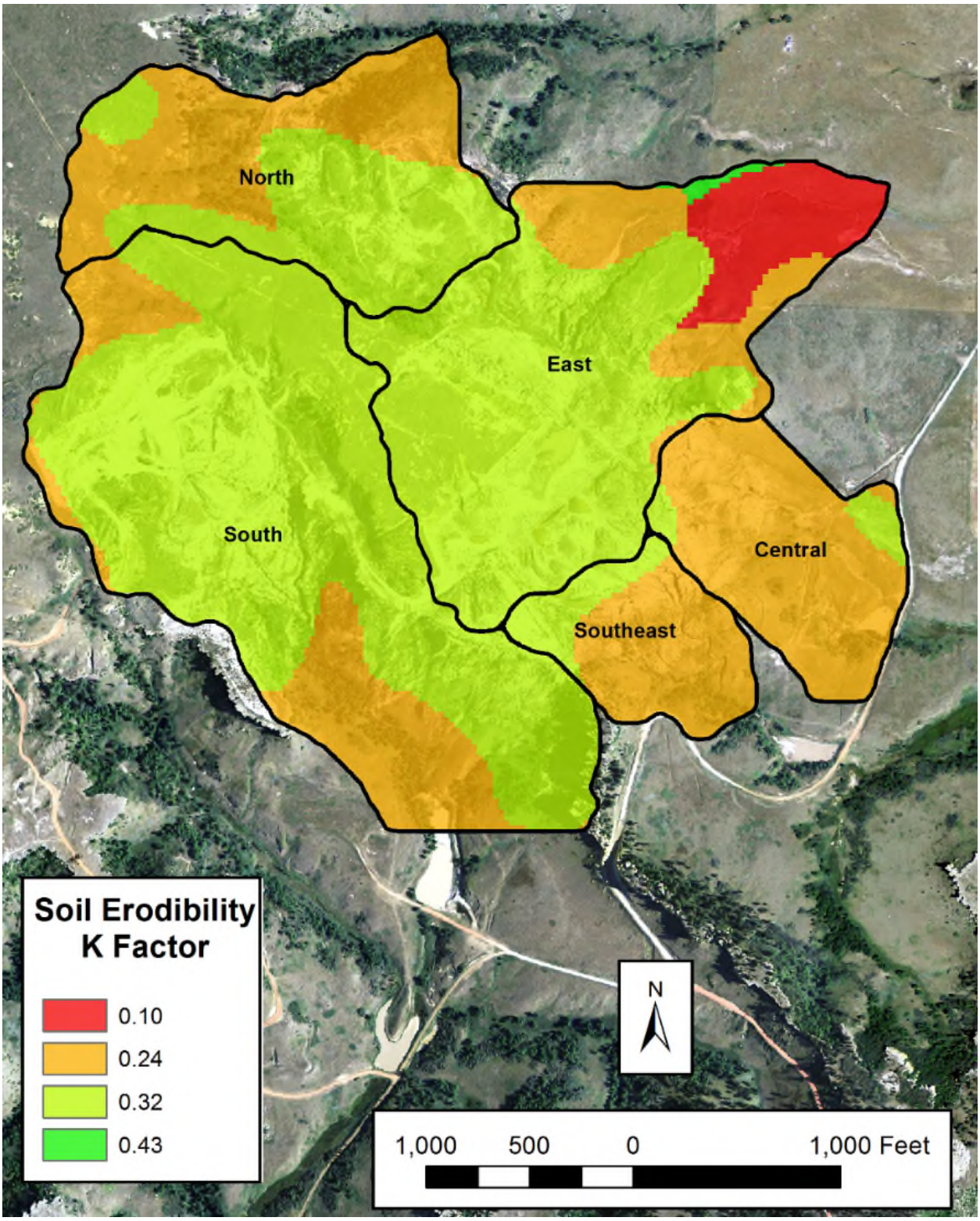

Figure 13 K Factor Map for Bluff B

3.3.4 Topographic Factor, LS Factor

The topographic factors of the RUSLE model include the slope length factor (L) and the slope gradient factor (S). The L and S factors represent the effects of slope length (L) and slope steepness (S) on the erosion of a slope. The combination of the two factors is commonly called the "topographic factor." The L factor is the ratio of the horizontal slope length to the experimentally measured slope length of 22.1 meters. The S factor is the ratio of the actual slope to an experimental slope of 9 percent. The L and S factors are designed such that they are one when the actual slope length is 22.1 and the actual slope is 9 percent. Programmatic methods for calculation

The slope length, L, topographic calculations for the RUSLE are as follows (Kim, et al., 2006) (Oliveira, et al., 2013):

$$L = \left(\frac{\lambda}{22.1}\right)^{m}$$

Where,

L is the slope length factor,
λ is the horizontal plot length and,
m is a variable exponent calculated from the ratio of rill-to-interrill erosion

Depending on the measured slope gradient, a different equation for S must be used. Choosing S allows the RUSLE to be more finely tuned for different terrains and is important because the topographic factor (and the RUSLE entirely) is very sensitive to the slope factor S. The slope factor S can be calculated as follows:

$$S = 10.8 \sin\theta + 0.03, \quad \text{slope gradient} \leq 9\%$$
$$S = 16.8 \sin\theta - 0.50, \quad \text{slope gradient} > 9\%$$

Where,

S is the slope factor, and
θ is the slope angle.

A GIS analysis was performed to estimate the LS factor using the digital elevation model for the site. Methods presented in Pelton e al. (2012) were followed to generate the spatial varying LS values for the watershed areas, as shown in Figure 14.

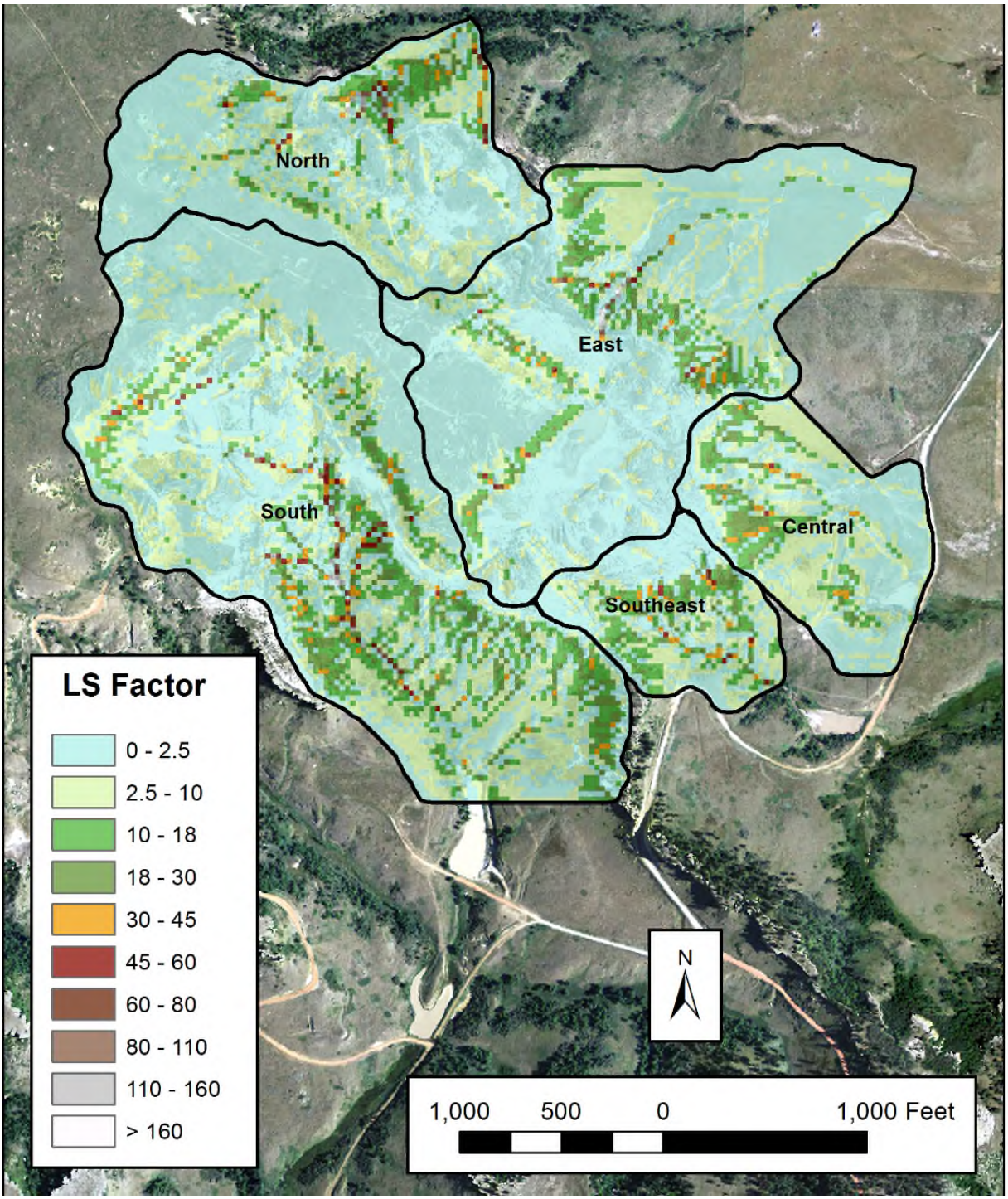

Figure 14 LS Factor Map for Bluff B

3.3.5 Cover Management, C Factor

The cover management factor (C-Factor) was presented in Equation 1 in Section 2.3.3. The C factor represents the effects of vegetation, management, and erosion-control practices on soil loss (Toy et al., 1998). The C factor represents the effect of plants, soil covers, soil biomass, and soil disturbing activities on soil loss and is the cropping management factor normalized to a tilled area with continuous fallow (Julien, 2010). A time-invariant option was followed for this model which assumes the C factor remains constant or does not change sufficiently over time to change soil-loss rates. The C factor values used for this analysis ranged between 0.035 and 0.45 and are based on values presented in Julien (2010) and modified from Wischmeier et al. (1978). Aerial imagery of the site from airplane flyovers, observations from site visits, and UAV surveys were used to determine the C factor for the study area. An example aerial image is provided in Figure 15; this image shows the approximate extent of the Southeast watershed taken from a UAV survey at the study area; the two different C factors are shown for this watershed. The C factor of 0.041 overlays the area where there are trees but not appreciable low brush with an average drop fall height of 13 feet with 80 percent cover that contacts the soil surface-percent ground cover (Julien, 2010). Similarly, the 0.45 C factor represents areas with no appreciable canopy. Figure 16 provides the spatial distribution of C factor values used for the GIS application of the RUSLE model.

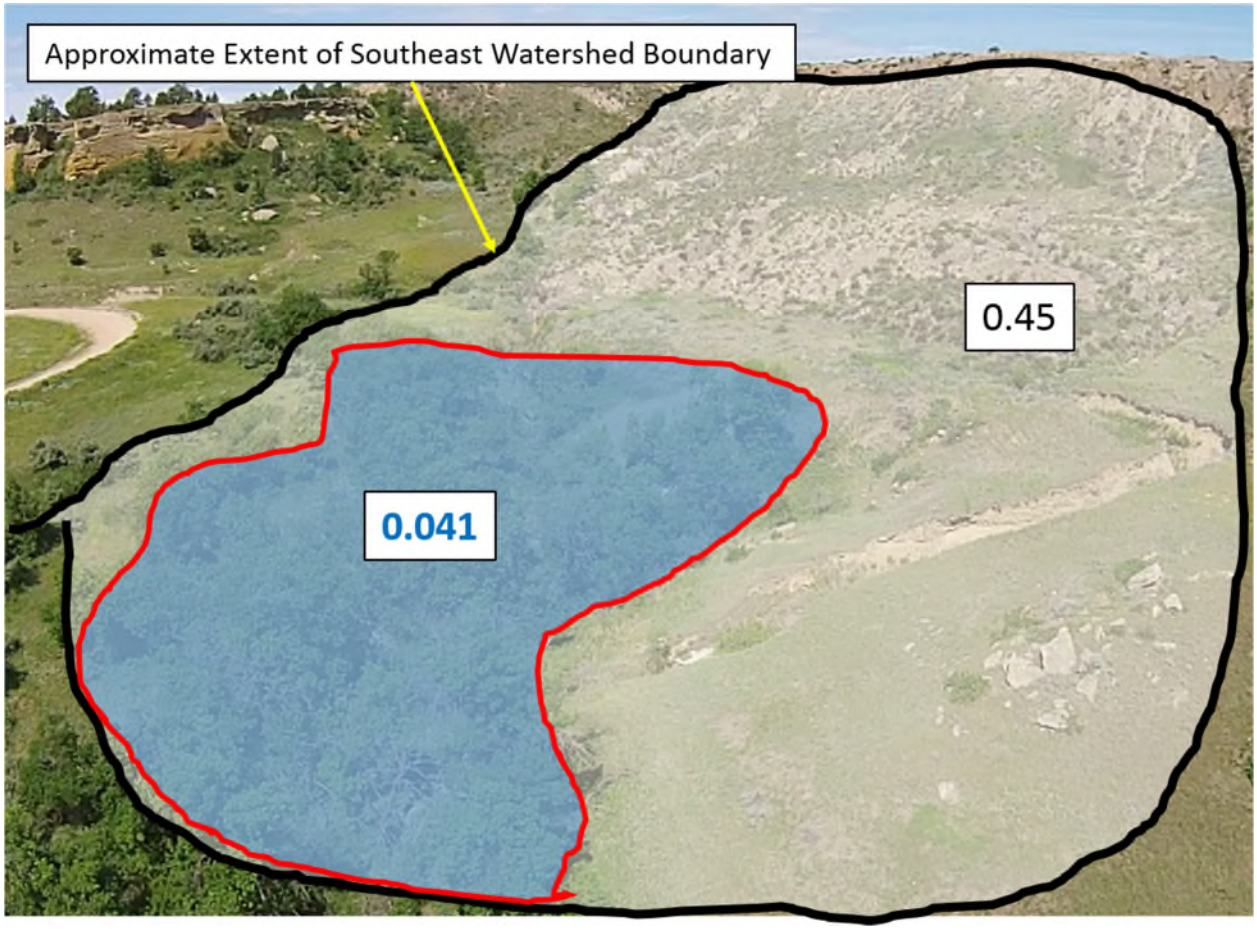

Figure 15 Aerial Image Obtained from UAV Survey Showing Crop Management, C Factor

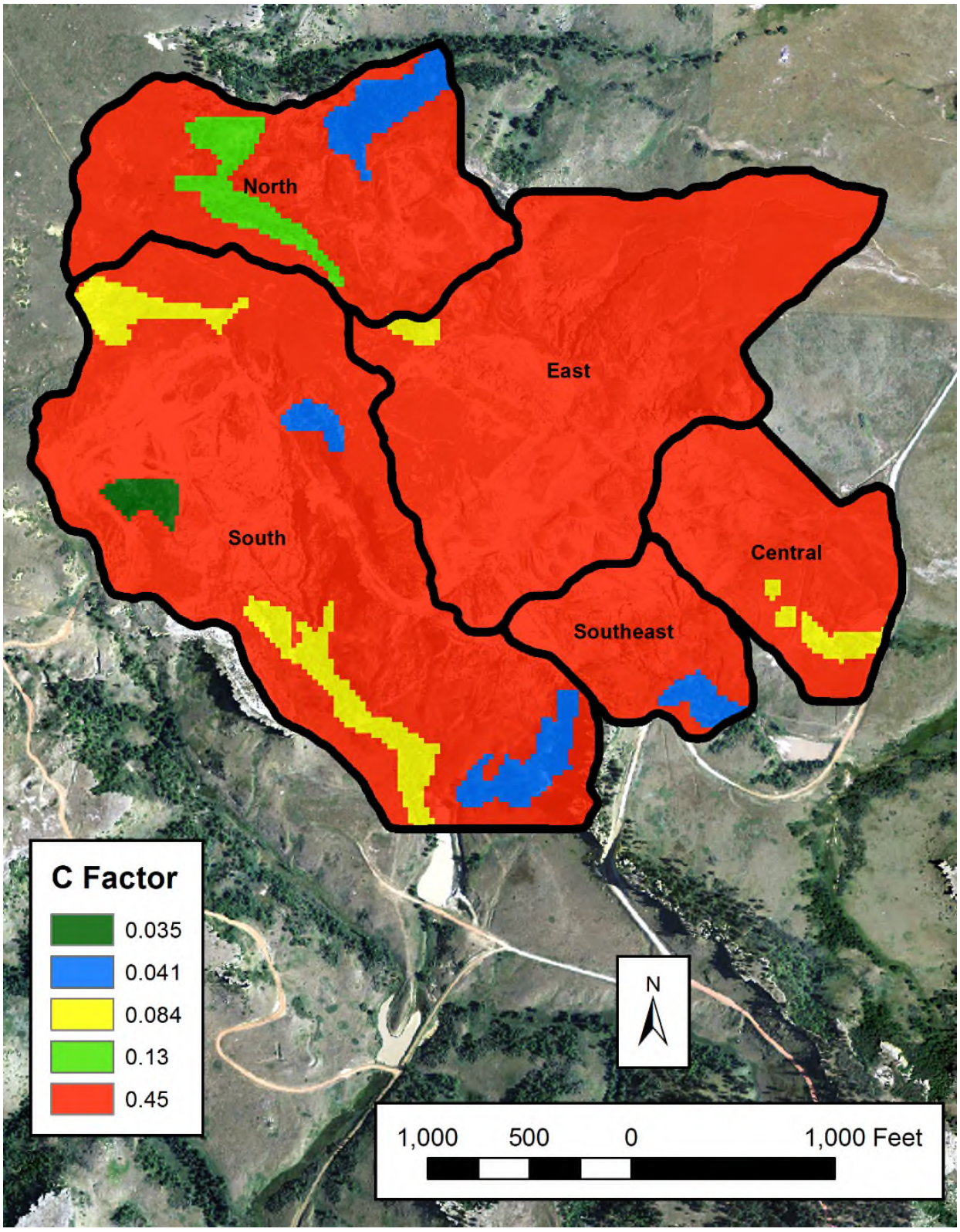

Figure 16 C Factor Map for Bluff B

3.3.6 Annual Gross Soil Loss, A

Using the parameters shown in Section 3.3.2 through 3.3.5, an analysis is performed using map algebra in GIS to estimate the average erosion in tons per year for each grid. A graphic illustrating the different raster data sets for each parameter overlain on the digital elevation model is shown in Figure 17. The average erosion in tons per acre per year is calculated for each grid; however, an additional multiplication factor to convert to tons per year for each grid is applied using the surface area of each grid. The results for the gross erosion modeling is presented in Section 4.2.1.

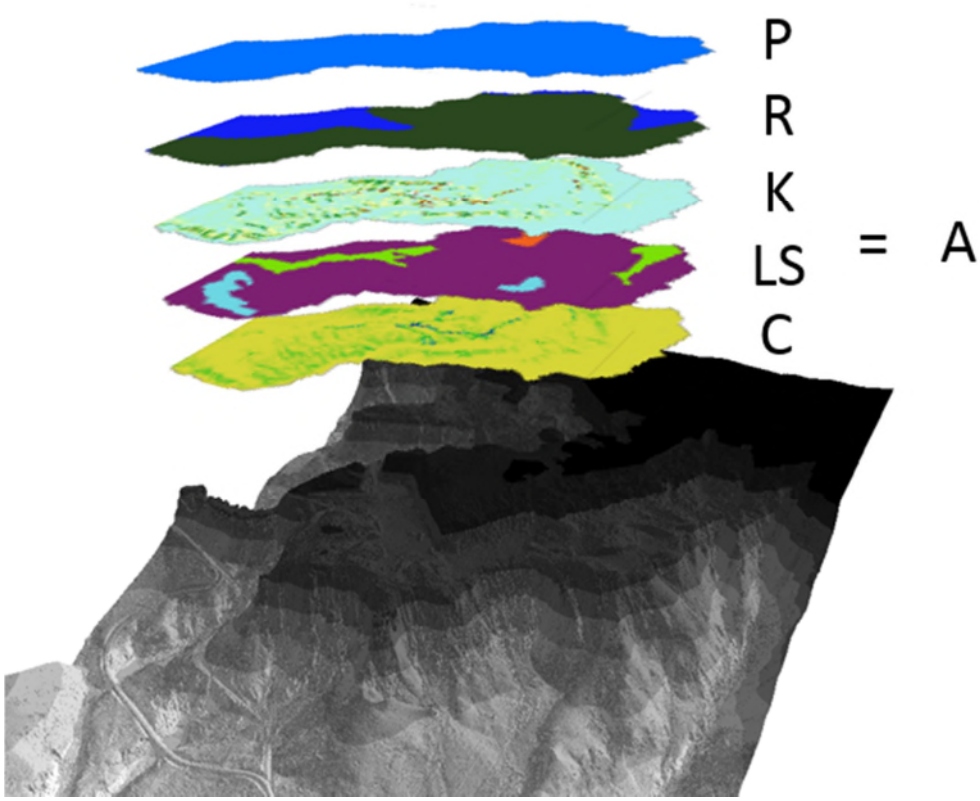

Figure 17 GIS Application of RUSLE

4.0 RESULTS

4.1 SOIL CONTAMINANT MAPPING

The methodology for collecting data for the soil contaminant mapping was presented in Section 3.1. Using the geostatistical techniques discussed earlier, soil contaminant maps were developed within the five watersheds of interest. The following subsections present the spatial extent of soil contamination for arsenic, uranium, and radium-226.

4.1.1 Arsenic Mapping

The spatial extent of arsenic contamination in surface soils within the five watersheds is provided in Figure 18. No data are available for some regions, and these areas are assumed not to contribute any transport of mass contaminants. This assumptions is valid for the South, Southeast, and Central watershed areas because the areas where there are no data appear to be in background areas with lower contaminant concentrations. However, it is likely that there is more contamination in the North and East watershed areas where no data are available. Therefore, the contaminant model likely underestimates the mass of contaminants in those northern watersheds.

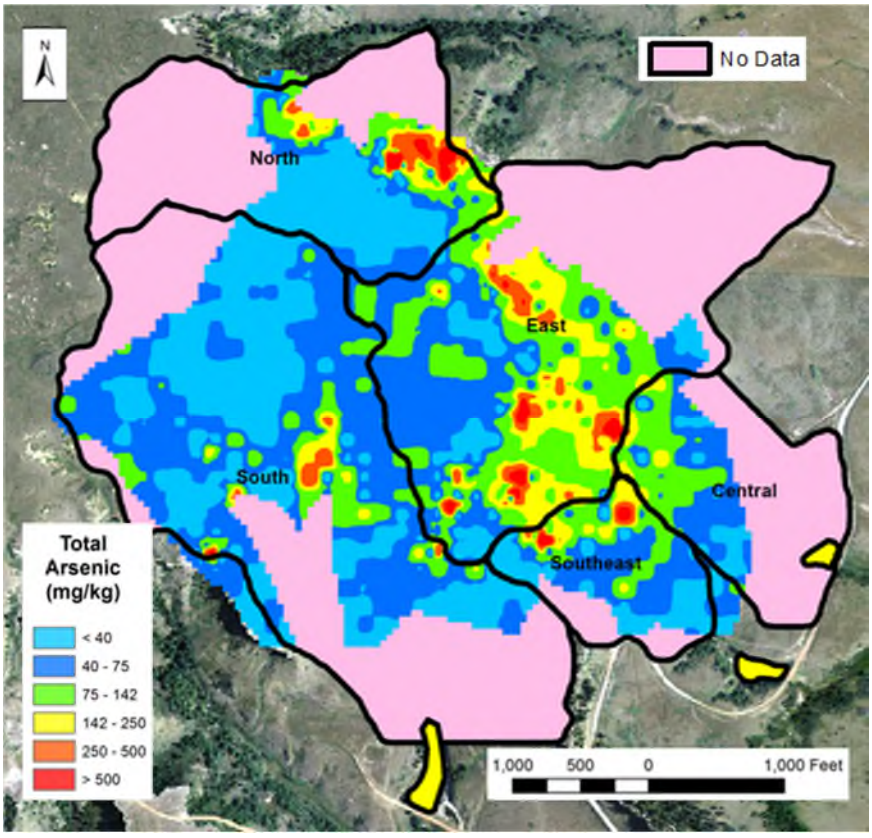

Figure 18 Soil Arsenic Concentration Map at Bluff B

4.1.2 Uranium Mapping

The spatial extent of uranium contamination in surface soils within the five watersheds is provided in Figure 19.

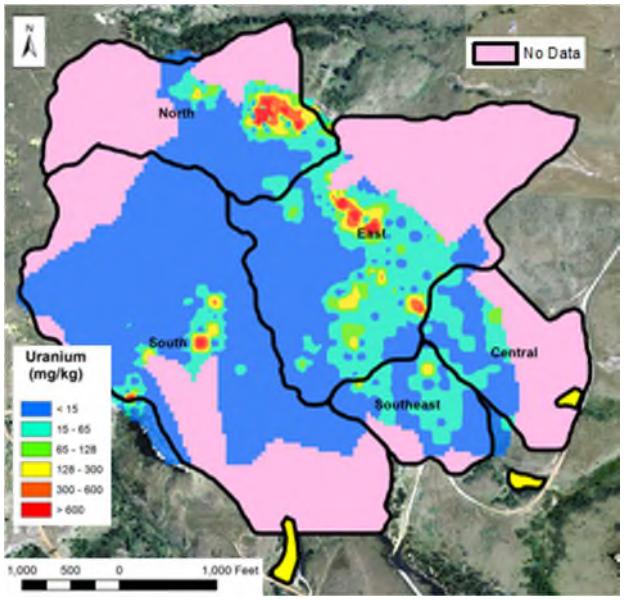

Figure 19 Soil Uranium Concentration Map at Bluff B

4.1.3 Radium Mapping

The spatial extent of radium-226 contamination in surface soils within the five watersheds is provided in Figure 20.

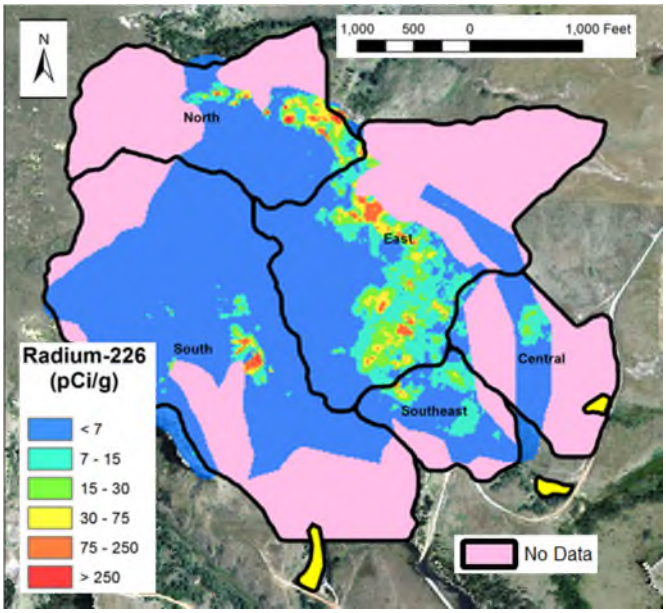

Figure 20 Soil Radium-226 Concentration Map at Bluff B

4.2 EROSION MAPPING

This section presents the erosion mapping results including the annual gross erosion, annual sediment yield, annual specific degradation, and contaminant transport analysis results of the GIS based erosion and contaminant models.

4.2.1 Annual Gross Erosion Results

Soil erosion mapping was performed following the methods outlined in Section 3.3 using a GIS application of RUSLE. A detailed analysis was performed on each watershed individually using the RUSLE parameters on a 26-foot x 26 -foot grid size. Overall, the highest annual gross erosion rate (A_T) was observed at the South watershed with an A_T of 3,366 tons per year. A total of 7,210 tons per year (6,540,979 kilograms [kg]/year) was estimated for all of the watersheds. Table 3 provides the summary results of the annual gross erosion for each watershed.

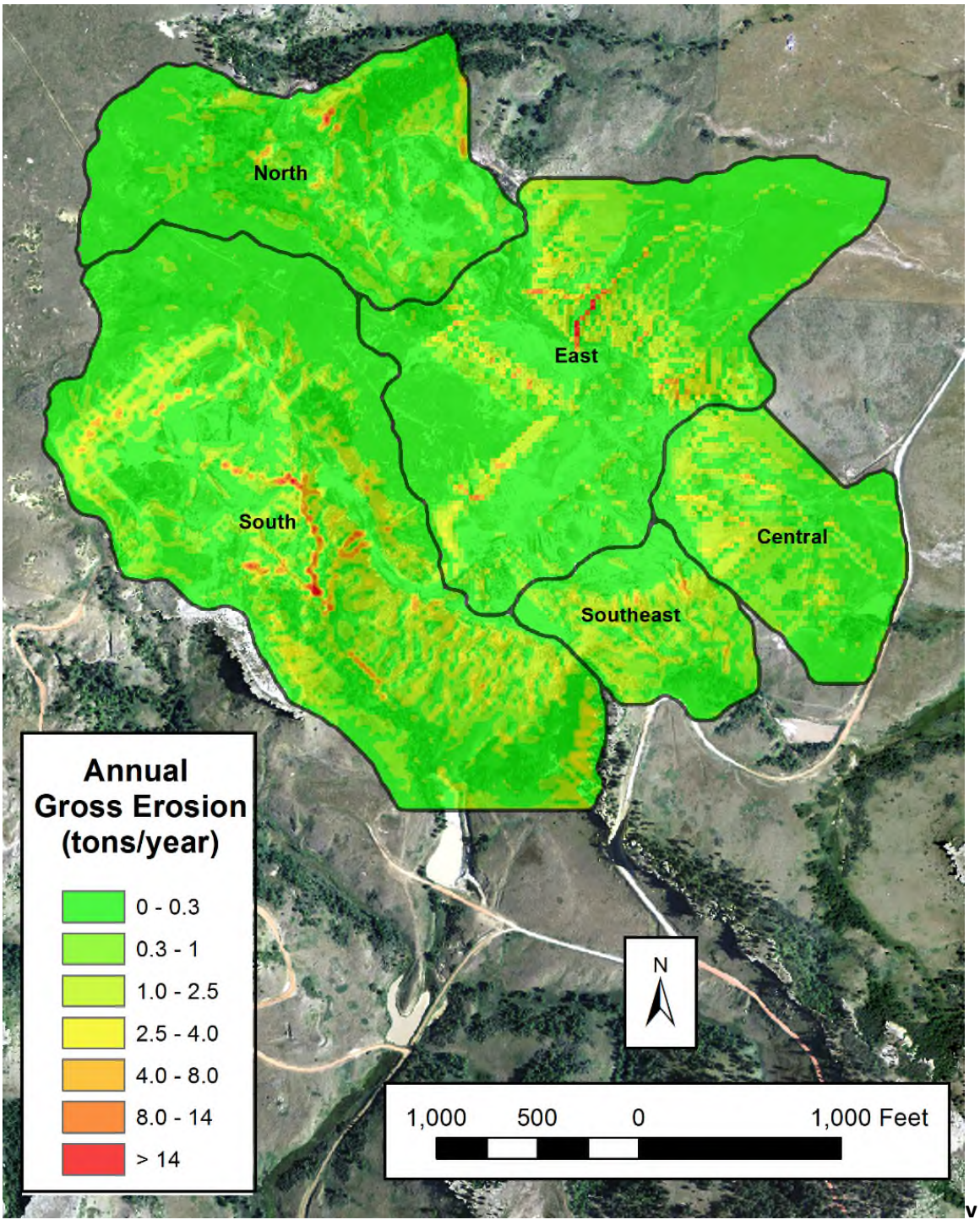

Figure 21 provides a color coded map showing the spatial extent of annual gross erosion at Bluff B.

Table 3 Summary of Annual Gross Erosion at Bluff B

Watershed ID	Gross Erosion, A_T	Gross Erosion, A_T
	tons/year	kg/year

North	713	646,462
East	1,836	1,665,793
Southeast	587	532,348
Central	708	642,444
South	3,366	3,053,933
Total	7,210	6,540,979

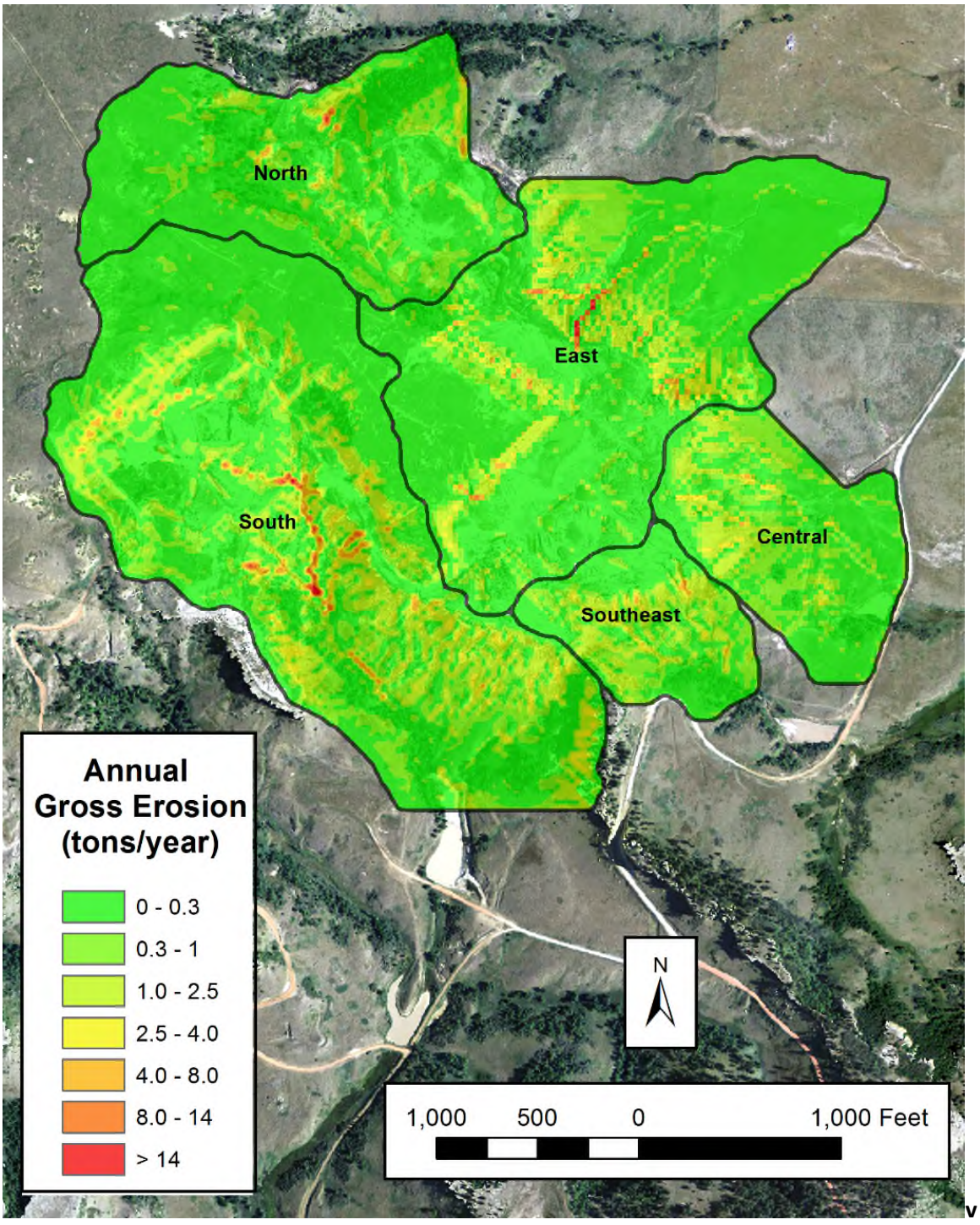

Figure 21 Annual Gross Erosion Map

4.2.2 Annual Sediment Yield Results

Sediment yield should not be confused with erosion. The rate sediment is carried by natural streams is usually less than the gross erosion on its upstream watershed (Julien, 2010). The sediment delivery ratio, S_{DR}, denotes the ratio of the sediment yield, Y, at a given stream cross-section to the gross erosion, A_T, from the watershed upstream of the measuring point (Julien, 2010). The spatial distribution of the annual gross erosion for the five watersheds draining Bluff B are presented on

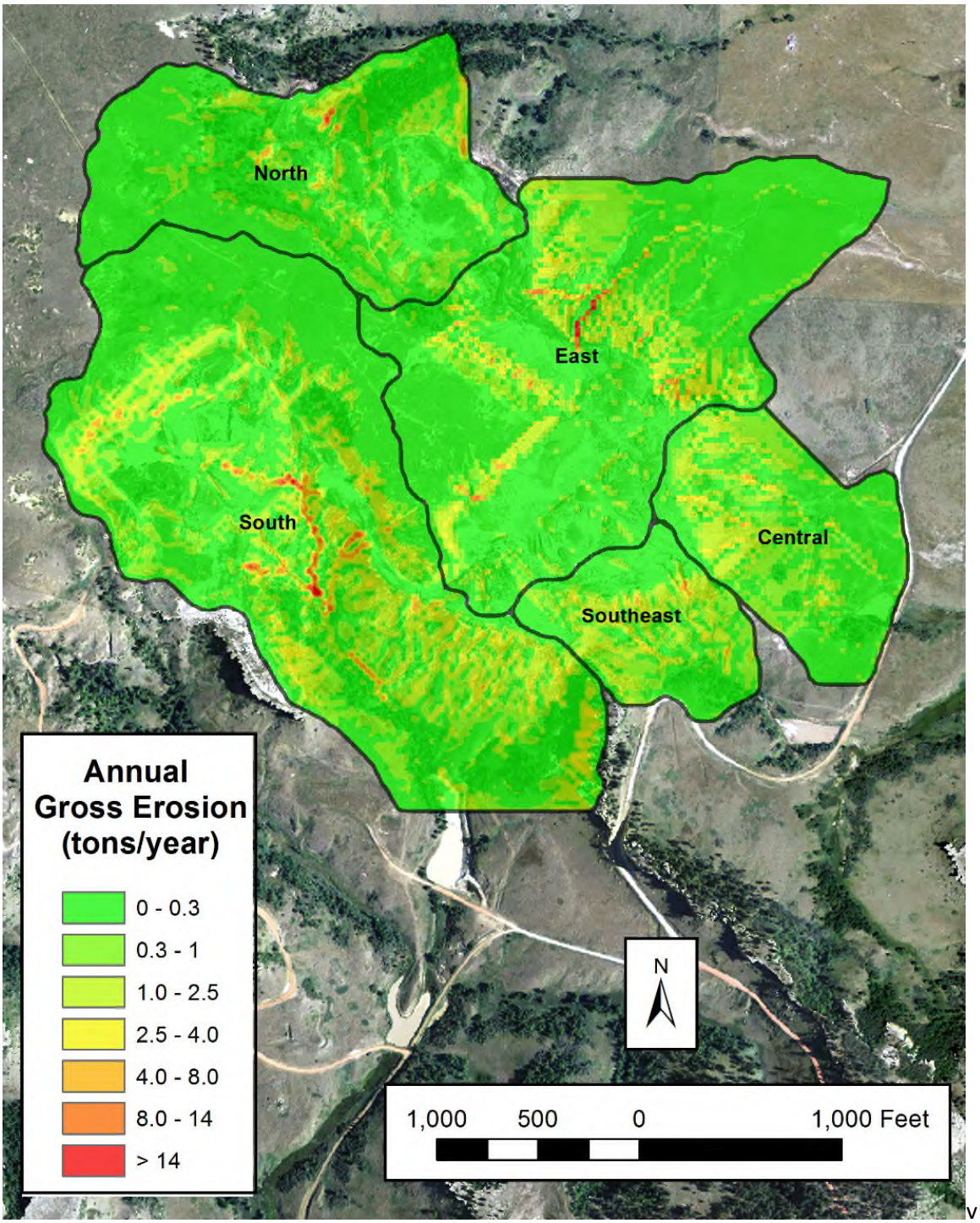

v

Figure 21 in Section 4.2.1. As presented in Section 0, numerous methods are available to estimate the S_{DR} of a particular watershed, and this parameter depends primarily on the drainage area, A, of the upstream watershed. Three different sediment delivery ratio methods were used, as shown in Equation 3 through Equation 4 in Section 0. The Boyce (1975), SCS (1978), and Vanoni (1975) sediment delivery ratio methods were evaluated. The SDR values obtained from these three methods is presented in Table 4 below. The highest variability (26 percent) of the SDR between the three methods was observed in the Southeast watershed.

Table 4 Sediment Delivery Ratio Results

Watershed ID	Area	Sediment Delivery Ratio, SDR		
	(km^2)	Boyce	SCS	Vanoni
North	0.17	0.69	0.69	0.59
East	0.29	0.59	0.65	0.55
Southeast	0.07	0.93	0.76	0.67
Central	0.10	0.82	0.73	0.63
South	0.38	0.55	0.63	0.53

Using the results from the RUSLE model, the annual gross erosion for each watershed was converted into sediment yield (Y) using Equation 3 through Equation 4 for each SDR method described above for each of the five watersheds of the study area. The sediment yield results varied based on different SDR equations. Table 5 presents the watershed area and sediment yield (in U.S. tons per year) for each wastershed using the different three sediment delivery ratios. The average sediment yield of all the methods ranged between 461 tons/year in the Southeast watershed to 1,920 tons/year in the south watershed. There is no spatial distribution of sediment yield similar to the grid-based annual gross erosion map presented in

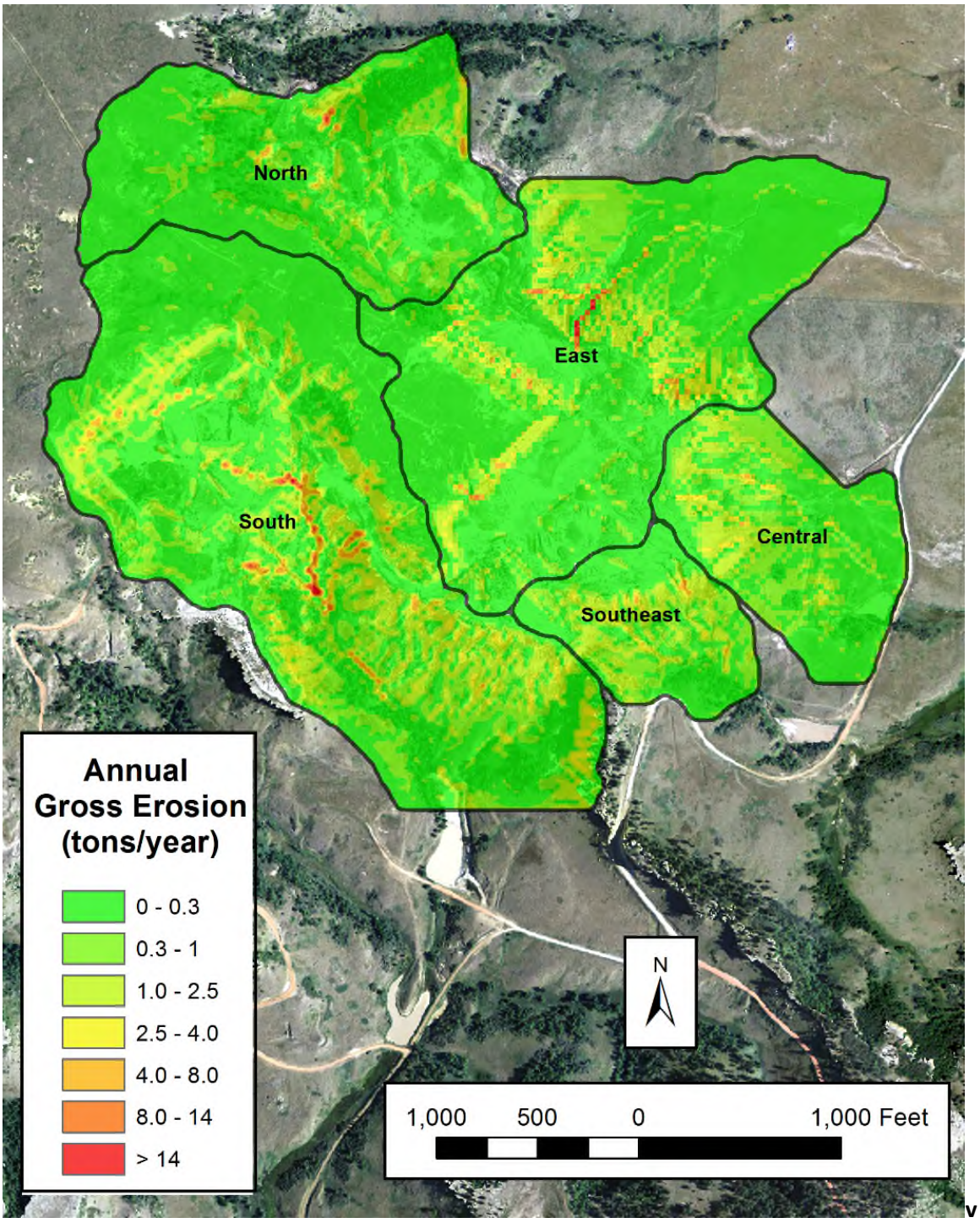

Figure 21.

Table 5 Sediment Yield Results

Watershed ID	Area	Sediment Yield (U.S. tons/year)			
	(km^2)	Boyce	SCS	Vanoni	Average

North	0.17	495	490	420	*468*
East	0.29	1,089	1,190	1,013	*1,097*
Southeast	0.07	545	449	390	*461*
Central	0.10	577	516	446	*513*
South	0.38	1,844	2,120	1,797	*1,920*

4.2.3 Annual Specific Degradation Results

The specific degradation for a given watershed is obtained by dividing the sediment yield, Y, by the drainage area, A, as described in Equation 5 of Section 2.3.4. The specific degradation is generally presented in a form of metric tons of sediment per year per area of watershed. Therefore, the sediment yield was converted into metric tons from U.S. tons and divided by the watershed area in km^2. Again, the specific degradation also varied based on the method utilized since multiple sediment delivery ratios were evaluated. The specific degradation rates for each watershed using three sediment delivery ratios are presented in Table 6. The average specific degradation that was calcuated using the various sediment delivery ratio methods ranged between 2,463 metric tons per km^2 per year and 6,396 metric tons per km^2 per year.

Table 6 Specific Degradation Results at Bluff B

Watershed ID	Area (km^2)	Specific Degradation (metric tons/km^2-year)			
		Boyce	SCS	Vanoni	Average
North	0.17	2,604	2,576	2,209	*2,463*
East	0.29	3,380	3,695	3,144	*3,407*
Southeast	0.07	7,558	6,219	5,412	*6,396*
Central	0.10	5,176	4,626	4,000	*4,601*
South	0.38	4,398	5,055	4,285	*4,579*

A study performed by Kane and Julien (2007) examined an extensive data set of sediment yield measurements on many reservoirs in the U.S. with various drainage areas. The results of the field measurements by Kane and Julien (2007) show a rather wide scatter of the data around mean values of serveral hundred metric tons per square kilometer and a decrease of specific degradation with drainage area (Julien 2010). The results of this study were plotted based on drainage area versus specific degradation to determine if similar patterns were observed at the study area. Figure 22 shows the specific degradation versus drainage area at the Riley Pass site on a semi-log plot. Overall, the results show that specific degradation decreases with drainage area, as can be seen with the left to right decreasing trendlines displayed on Figure 22 and follow the expected results from Kane and Julien (2007). Two of the smallest drainage areas at the site (Southeast and Central) have the two highest observed specific degradation rates. However, the three watersheds (North, East, and South) show an increase in specific degradation with drainage area. As noted in Julien (2010), there is a wide scatter of data around the mean values, and the results may be representative of actual erosion conditions occurring at the study area.

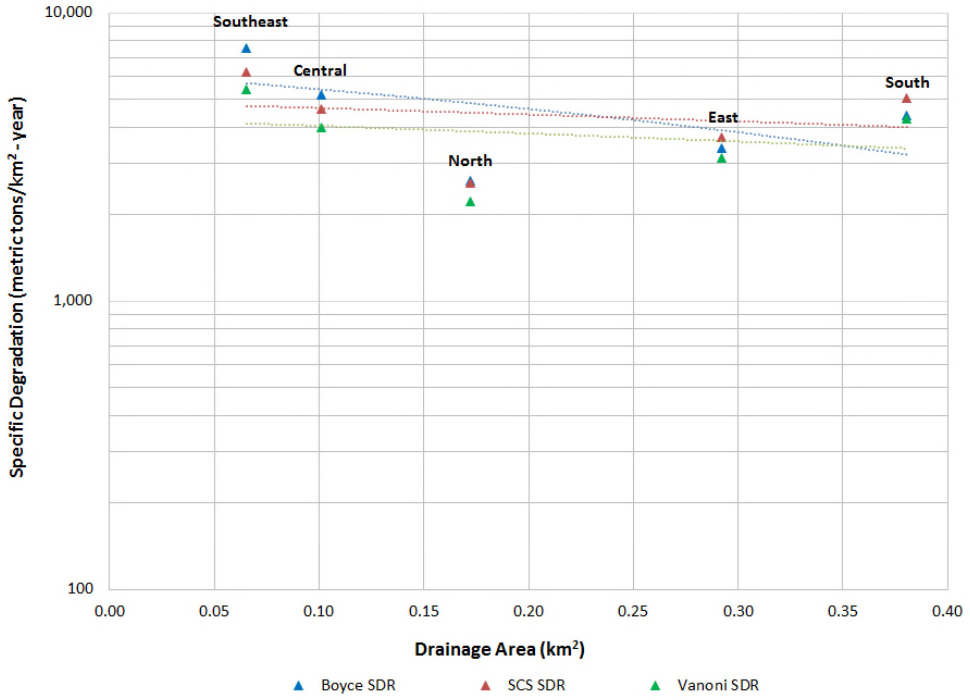

Figure 22 Specific Degradation vs. Drainage Area at Riley Pass w/Trendlines

An evaluation compared the results of this study with the reservoir sedimentation study of Kane and Julien (2007). Figure 23 through Figure 25 show the specific degradation rates for each drainage area for each sediment delivery ratio method used to determine sediment yield. The results are similar for all of the sediment delivery ratio methods applied. Overall, the results show that the Southeast, Central, and South watersheds fall outside of the 95 percent confidence interval of the Kane and Julien (2007) study, while the North and East results fall within the expected bounds of the specific degradation and drainage area relationship.

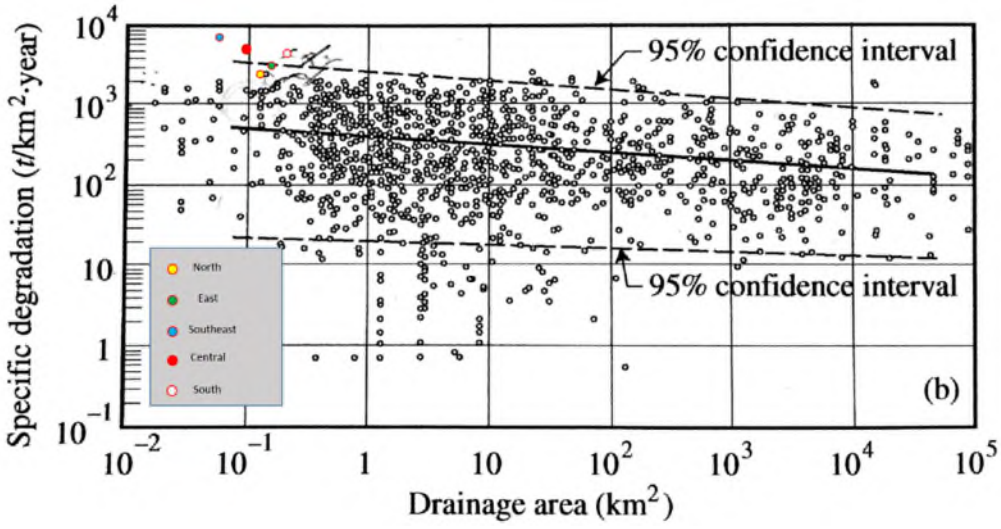

Figure 23 Specific Degradation vs. Watershed Area (Boyce SDR Method)

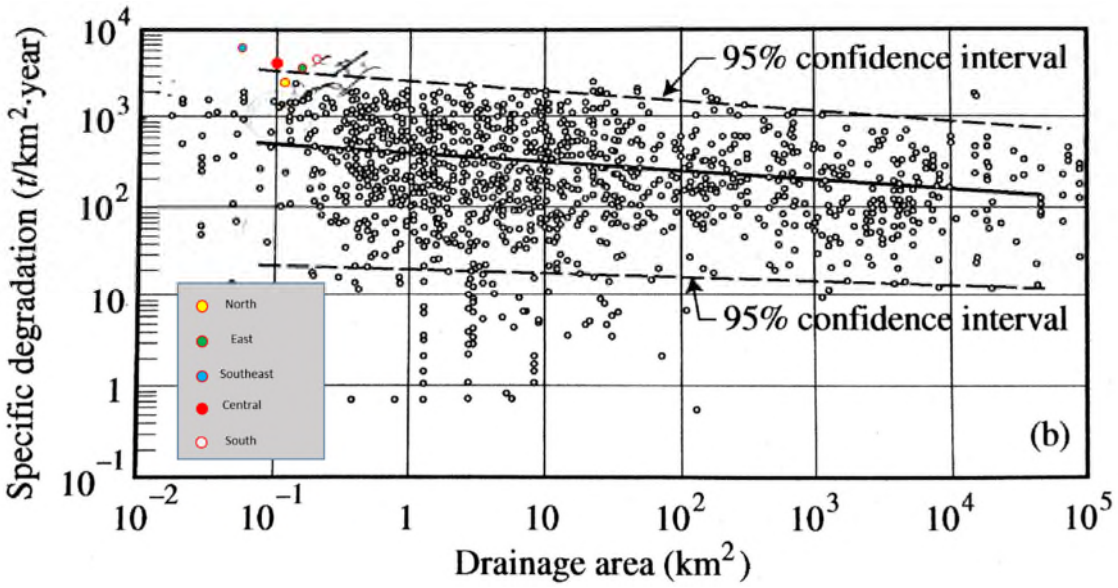

Figure 24 Specific Degradation vs. Watershed Area (SCS SDR Method)

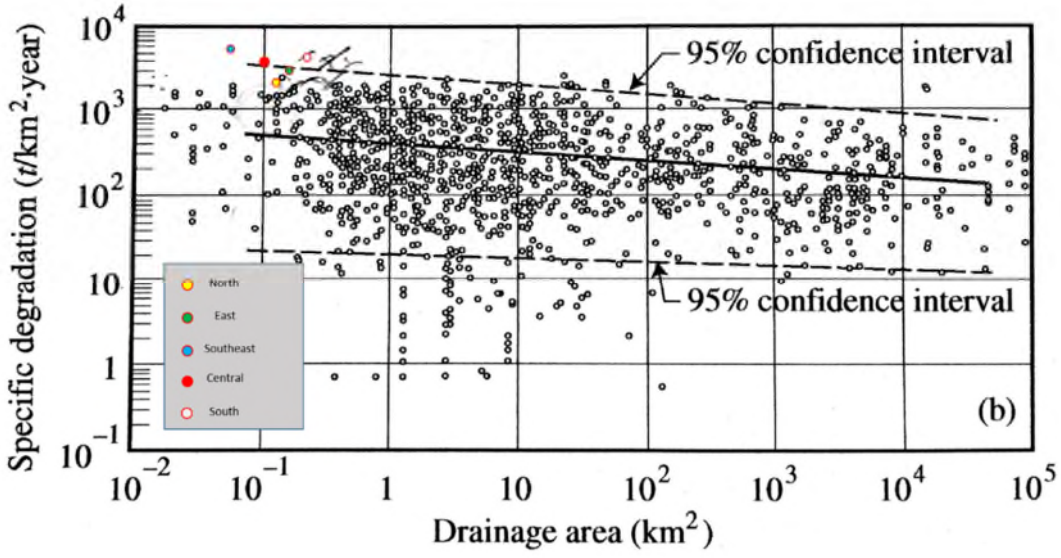

Figure 25 Specific Degradation vs. Watershed Area (Vanoni SDR Method)

The results of this study indicate the specific degradation calculated from the RUSLE model and the various sediment delivery ratio methods result in higher than expected (outside 95 percent confidence interval) rates for three of the drainage areas evaluated (Southeast, Central, and South) compared with what would be expected for an unimpacted watershed of the same size. This phenomenon is attributed to the strip mining that occurred at the site and the extensive land deterioration because of this type of mining. Julien (2010) states that, under some circumstances, the erosion rates from human activities (such as mining operations) can be 100 to 1,000 times greater than the geological erosion rate of 25 metric ton/km^2-year. The results from this study are relatively close to the upper limits for the Kane and Julien (2007) study; however, further information must be researched to determine the extent of mining in the drainage areas evaluated during the Kane and Julien (2007) study.

While the results of this study may seem outside of the limits of previous studies, data are available to validate these results. An analysis was performed to evaluate the results of this study and compare with available site data for sediment volume removal that occurred on two separate occasions within the past two decades at the study area. Coincidently, annual sediment yield data are available for the three study areas (Southeast, Central, and South) that exhibited specific degradation rates outside of the expected ranges. Section 5.0 presents the data validation results using site-specific sediment yield from the study area.

4.2.4 Contaminant Transport Analysis

The final objective of this study is to evaluate the mass (or activity) and concentration of arsenic, uranium, and radium-226 that is being transported off-site from each of the watersheds. Using the results from the soil contaminant mapping analysis (Section 4.1), a GIS analysis was performed to calculate the amount or activity and concentration of sediment for each of the contaminants that is being transported off-site. Estimates of annual soil erosion loss for arsenic, uranium, and radium-226 were calculated using the soil contaminant mapping and gross erosion results from the RUSLE model. After the optimal geostatistical model was selected for each set of contaminant data using the Geostatistical Analyst tool in ArcGIS 10.1, continuous raster surfaces were generated using the same resolution as the RUSLE parameters. These rasters were snapped to the original DEM to allow for ease of map algebra between the data sets. The resulting annual gross erosion, A, for each grid was converted into kg/year (or pCi/year for radium-226) and multiplied against the arsenic and uranium contaminant grid in mg/kg and pCi/g for radium-226, resulting in a final grid of annual gross erosion of arsenic in mg/year, uranium in mg/year, and radium-226 in pCi/year. The data were then exported and analyzed in a spreadsheet for each contaminant for each watershed. For presentation, the values were converted to tons per year of arsenic and uranium and pCi/year for radium-226 for each watershed. Table 7 below presents the annual gross erosion for arsenic for each watershed. The annual gross erosion from arsenic is estimated at 0.366 ton per year for all of the watersheds. The East and South watersheds have the highest annual gross erosion for arsenic.

Table 7 Annual Gross Erosion for Arsenic at Bluff B

Watershed ID	Gross Erosion, Arsenic	Gross Erosion, Arsenic
	mg/year	tons/year
North	23,961,213	0.026
East	124,078,568	0.137
Southeast	31,455,492	0.035
Central	34,002,169	0.037
South	118,563,605	0.131
Total	332,061,047	0.366

The annual gross erosion from uranium is estimated at 0.146 ton per year for all of the watersheds. The East and South watersheds have the highest annual gross erosion for uranium. Table 8 below presents the annual gross erosion for uranium for each watershed.

Table 8 Annual Gross Erosion for Uranium at Bluff B

Watershed ID	Gross Erosion, Uranium	Gross Erosion, Uranium
	mg/year	tons/year
North	15,621,507	0.017
East	70,060,906	0.077
Southeast	6,546,025	0.007
Central	7,910,215	0.009
South	32,411,174	0.036
Total	132,549,827	0.146

Radium-226 is measured as a mass activity ratio (pCi/g), and therefore the total activity in pCi is estimated rather than the mass of radium-226. The annual gross erosion is 0.027 curies per year. The East and South watersheds have the highest annual gross erosion for radium-226. Table 9 below presents the annual gross erosion in activity for radium-226 for each watershed.

Table 9 Annual Gross Erosion for Radium-226 at Bluff B

Watershed ID	Gross Erosion, Ra-226	Gross Erosion, Ra-226
	pCi/year	Ci/year
North	2,547,083,035	0.0025
East	8,641,203,871	0.0086
Southeast	2,249,324,147	0.0022
Central	1,062,928,208	0.0011
South	12,543,131,427	0.0125
Total	27,043,670,688	0.0270

Not all of the sediment loss calculated from the gross erosion will be carried out of the watershed by the drainage channels; therefore, sediment is deposited between the source and the stream whenever the transport capacity of runoff water is insufficient to sustain transport (Julien, 2010). As a result, a sediment yield analysis is required to estimate the amount of soil and contaminants that will be transported out of each watershed. Using the sediment delivery ratio from Vanoni (1975), the sediment yield is calculated for each of the contaminants of concern providing a better estimate for actual total material being transported off site. The total sediment yield of the contaminant of concern is then divided by the total sediment yield to obtain an estimated sediment concentration for arsenic, uranium, and radium-226. Table 10 through Table 12 present the sediment yield and predicted sediment concentrations arsenic, uranium, and radium-226. The results of this analysis show that the highest arsenic, uranium, and radium-226 concentrations all reside in the East watershed.

Table 10 Sediment Yield and Predicted Sediment Concentration of Arsenic

Watershed ID	Sediment Yield (Total Sediment) [kg/year]	Sediment Yield (Arsenic) [mg/year]	Predicted Sediment Concentration (Uranium) [mg/kg]
North	3.81E+05	1.4.E+07	37
East	9.19E+05	6.8.E+07	74
Southeast	3.54E+05	2.1.E+07	59
Central	4.05E+05	2.1.E+07	53
South	1.63E+06	6.3.E+07	39

Table 11 Sediment Yield and Predicted Sediment Concentration of Uranium

Watershed ID	Sediment Yield (Total Sediment) [kg/year]	Sediment Yield (Uranium) [mg/year]	Predicted Sediment Concentration (Uranium) [mg/kg]
North	3.81E+05	9.2.E+06	24
East	9.19E+05	3.9.E+07	42
Southeast	3.54E+05	4.4.E+06	12
Central	4.05E+05	5.0.E+06	12
South	1.63E+06	1.7.E+07	11

Table 12 Sediment Yield and Predicted Sediment Concentration of Radium-226

Watershed ID	Sediment Yield (Total Sediment) [g/year]	Sediment Yield (Radium-226) [pCi/year]	Predicted Sediment Concentration (Radium-226) [mg/kg]
North	3.81E+08	1.5.E+09	3.94
East	9.19E+08	4.8.E+09	5.19
Southeast	3.54E+08	1.5.E+09	4.23
Central	4.05E+08	6.7.E+08	1.65
South	1.63E+09	6.7.E+09	4.11

An evaluation was performed to assess how much contaminated sediment is transferred off site and how much is contained in the sediment ponds assuming 100 percent containment. Table 13 presents the results of this evaluation, showing that between 36 percent and 59 percent of the contaminants of concern are being adequately contained within the existing sediment control structures at the site.

Table 13 Sediment Transported Off-site Assessment for Contaminants of Concern

Contaminant	Units	Quantity Leaving Site	% Contained
Arsenic	lbs/year	415	56%
Uranium	lbs/year	164	36%
Radium-226	Ci/year	0.015	59%

5.0 FIELD DATA VALIDATION

Three primary validation methods are used to assess the RUSLE model and sediment contaminant concentration estimates presented in Section 4.0. These three methods include (1) calculation of sediment yield, (2) calculation of sediment delivery ratio, and (3) calculation of sediment contaminant concentrations. The calculated values from each of these methods were then compared and evaluated with respect to the associated parameters measured in the field (sediment yield and sediment concentration) or estimated using methods presented in the literature review (sediment delivery ratio). This section discusses the methodology and evaluation of the data validation analysis for sediment yield, sediment deliver ratio, and sediment contaminant concentrations used in validating the GIS-based models.

5.1 CALCULATION OF SEDIMENT YIELD

There are three sediment ponds (*identified as SP1, SP2, and SP3 in Figure 10)* providing sediment recovery and containment processes during storm events at the study area. These sediment ponds have been maintained over the years by removing the sediment trapped to maintain sediment trapping efficiency and achieve the original pond design objectives. Figure 26 provides an aerial view of sediment pond SP2. Historical sediment removal information in the form of construction field logs and contractor reports were obtained from the USFS. The three sediment ponds (SP1, SP2, and SP3) were evaluated for two different sediment removal events between 1997 and 2008. This information was used to estimate the volume of sediment removed from within each pond to estimate the sediment yield within each pond.

Figure 26 Aerial Image of Sediment Pond SP2

The information obtained from the ponds included measured wet sediment volume in cubic yards. The data were obtained from USFS contract documents from two major pond sediment removal events between 1997 and 2008. This information was used to estimate the annual sediment volume within sediment ponds SP1, SP2, and SP3. The measured total sediment volume ranged between 220 m^3/year in SP1 and 1,695 m^3/year in SP3.

Table 14 Summary of Measured Sediment Volume Removed from Ponds per Year

Sediment Pond ID	Measured Total Sediment Volume [V_T] (yd^3/year)[1]	Measured Total Sediment Volume [V_T] (m^3/year)
SP1	287	220
SP2	806	617
SP3	2,217	1,695

[1]Based on data obtained from USFS contract between 1997 and 2008

Geotechnical characteristics of the sediment trapped in ponds SP1, SP2, and SP3 were available from a historical study performed at each pond. Literature-reported values of submerged sediment in saturated and dried sediment deposits are presented in Julien (2010). Submerged sediment deposits tend to have a density of 70 pounds per cubic foot (lb/ft^3) (1,122 kilograms per cubic meter [kg/m^3]). The physical properties and sediment particle analysis was available for SP1, SP2, and SP3. The sediment ponds SP2 and SP3 consisted of a soft clay material, and SP1 consisted of a loose angular-grained silty sand. A value of 1,121 kg/m^3 was used for sediment ponds SP2 and SP3. Based on the material characteristics of SP1, a more dense value of 1,632 kg/m^3 obtained for typical silty-sand sediment from Das (2000) was used for SP1. The relationship between sediment density (ρ_d) and mass of solid sediment (M_S) and total volume of sediment (V_T) is as follows:

$$\rho_d = \frac{M_S}{V_T} \therefore$$

$$M_S = \rho_d V_T$$

The sediment yield is derived from the measured sediment volume for each pond as follows:

For SP1 $$M_S = \left(1{,}632\ \frac{kg}{m^3}\right) \times (220\ m^3) \times \left(\frac{1\ US\ ton}{907.185\ kg}\right) = 395\ {US\ tons}/{year}$$

For SP2 $$M_S = \left(1{,}122\ \frac{kg}{m^3}\right) \times (617\ m^3) \times \left(\frac{1\ US\ ton}{907.185\ kg}\right) = 762\ {US\ tons}/{year}$$

For SP3 $$M_S = \left(1{,}122\ \frac{kg}{m^3}\right) \times (617\ m^3) \times \left(\frac{1\ US\ ton}{907.185\ kg}\right) = 2{,}095\ {US\ tons}/{year}$$

The measured sediment yield ranged between 395 US tons/year for SP1 and 2,095 US tons/year for SP3. The measured sediment yield results were compared with the predicted sediment yield results that were determined using the different sediment deliver ratio methods (Boyce, SCS, and Vanoni). Table 15 provides the measured sediment yield, predicted sediment yield, and the percent difference for the three ponds using the Boyce sediment delivery ratio method. The percent difference ranged between 13 percent and 38 percent.

Table 15 Measured vs Predicted Sediment Yield (Boyce Method)

Sediment Pond ID	Measured Sediment Yield (U.S. tons/year)	Estimated Sediment Yield (U.S. tons/year) from Boyce SDR Method	Percent Difference
SP1	395	577	38%
SP2	762	545	33%
SP3	2,095	1,844	13%

Table 16 provides the measured sediment yield, predicted sediment yield, and the percent difference for the three ponds using the SCS sediment delivery ratio method. The percent difference ranged between 1 percent and 52 percent.

Table 16 Measured vs Predicted Sediment Yield (SCS Method)

Sediment Pond ID	Measured Sediment Yield (U.S. tons/year)	Estimated Sediment Yield (U.S. tons/year) from SCS SDR Method	Percent Difference
SP1	395	516	27%
SP2	762	449	52%
SP3	2,095	2,120	1%

Table 17 provides the measured sediment yield, predicted sediment yield, and the percent difference for the three ponds using the Vanoni sediment delivery ratio method. The percent difference ranged between 12 percent and 65 percent.

Table 17 Measured vs Predicted Sediment Yield (Vanoni Method)

Sediment Pond ID	Measured Sediment Yield (U.S. tons/year)	Estimated Sediment Yield (U.S. tons/year) from Vanoni Method	Percent Difference
SP1	395	446	12%
SP2	762	390	65%
SP3	2,095	1,797	15%

Table 18 provides the measured sediment yield, predicted sediment yield, and the percent difference for the three ponds using the average from the three different sediment delivery ratio methods. The percent difference ranged between 15 percent and 65 percent.

Table 18 Measured vs Predicted Sediment Yield (Average of Boyce, SCS, Vanoni Methods)

Sediment Pond ID	Measured Sediment Yield (U.S. tons/year)	Estimated Sediment Yield (U.S. tons/year) Average from All Methods	Percent Difference
SP1	513	513	26%
SP2	461	390	65%
SP3	1,920	1,797	15%

Overall, there is strong agreement between the measured and predicted sediment yield for the three methods. Figure 27 presents the linear relationship between measured and predicted sediment yield for the three ponds using the three different SDR methods.

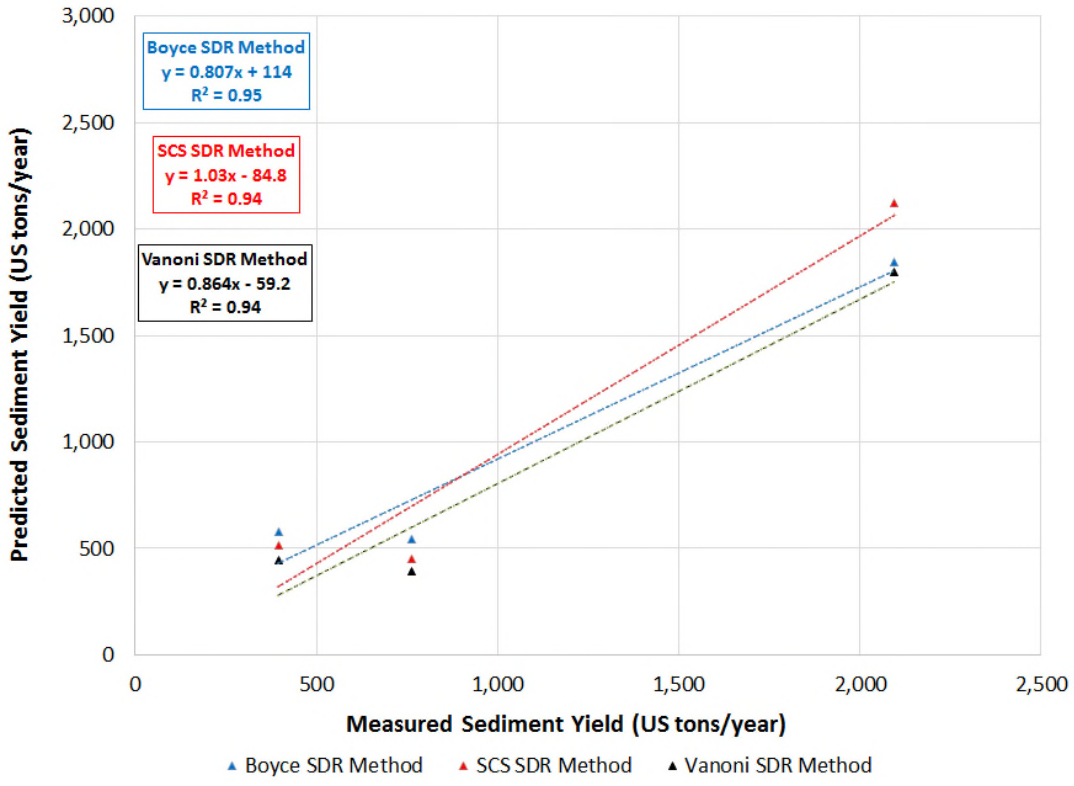

Figure 27 Measured vs Predicted Sediment Yield Based on SDR Method

Overall, the predicted sediment yield measurements from the RUSLE model and delivery ratio methods coincided with the measured sediment yields.

5.2 SEDIMENT DELIVERY RATIO

The measured sediment accumulation in reservoirs of known age and history is an excellent source of data for establishing sediment yield. The magnitude of the sediment delivery ratio for a particular basin will be influenced by a wide range of geomorphological and environmental factors, including the nature, extent, and location of the sediment sources, relief and slope characteristics, the drainage pattern and channel conditions, vegetation cover, land use and soil texture (Walling, 1983). Basin area has frequently been isolated as the dominant control mechanism for sediment delivery ratio, as was evidenced with three SDR methods used in Section 5.1 to estimate sediment yield from the gross erosion rate generated from the GIS based RUSLE model. An evaluation was performed to assess the sediment delivery ratio (SDR) using the measured sediment yield collected from the sediment ponds and the gross erosion results from the RUSLE soil loss equation. The SDR was calculated using Equation 2 in Section 2.3.4. These results are presented in Table 19 below. The sediment delivery ratio ranged between 0.56 and 1.30 for the three watershed areas draining into sediment ponds SP1, SP2, and SP3.

Table 19 Calculated Sediment Delivery Ratio Analysis Results

Sediment Pond ID	Gross Erosion [A_T] (U.S. tons/year)	Measured Sediment Yield [Y] (U.S. tons/year)	Sediment Delivery Ratio, SDR
SP1	708	395	0.56
SP2	587	762	1.30
SP3	3,366	2095	0.62

Table 20 shows the calculated SDR values compared with the estimated SDR values for each of the three SDR methods (Boyce, SCS, and Vanoni). The calculated SDR (0.56) for the Central watershed draining into SP1 was lower than the three methods. The calculated SDR (1.3) for the Southeast watershed draining into SP2 was higher than the three methods and was also greater than unity. However, values of delivery ratio in excess of 100 percent could be interpreted as reflecting short-term storage and remobilization during the delivery process, so that the sediment yield could exceed the estimate of gross erosion for a particular event (Walling, 1983). The calculated SDR (0.62) for the South watershed draining into SP3 was within the range of the three methods.

Table 20 Calculated Sediment Delivery Ratio Compared with Traditional Methods

Sediment Pond ID	Calculated Sediment Delivery Ratio [SDR]	Estimated SDR (Boyce)	Estimated SDR (SCS)	Estimated SDR (Vanoni)
SP1	0.56	0.82	0.73	0.63
SP2	1.30	0.93	0.76	0.67
SP3	0.62	0.55	0.63	0.53

The similarity between the calculated and estimated SDR values is shown based on watershed area vs. SDR value in Figure 28. Power regression relationships were derived for the three estimated SDR values (shown in three different colors) compared to the power relationship between the calculated SDR methods (shown in black).

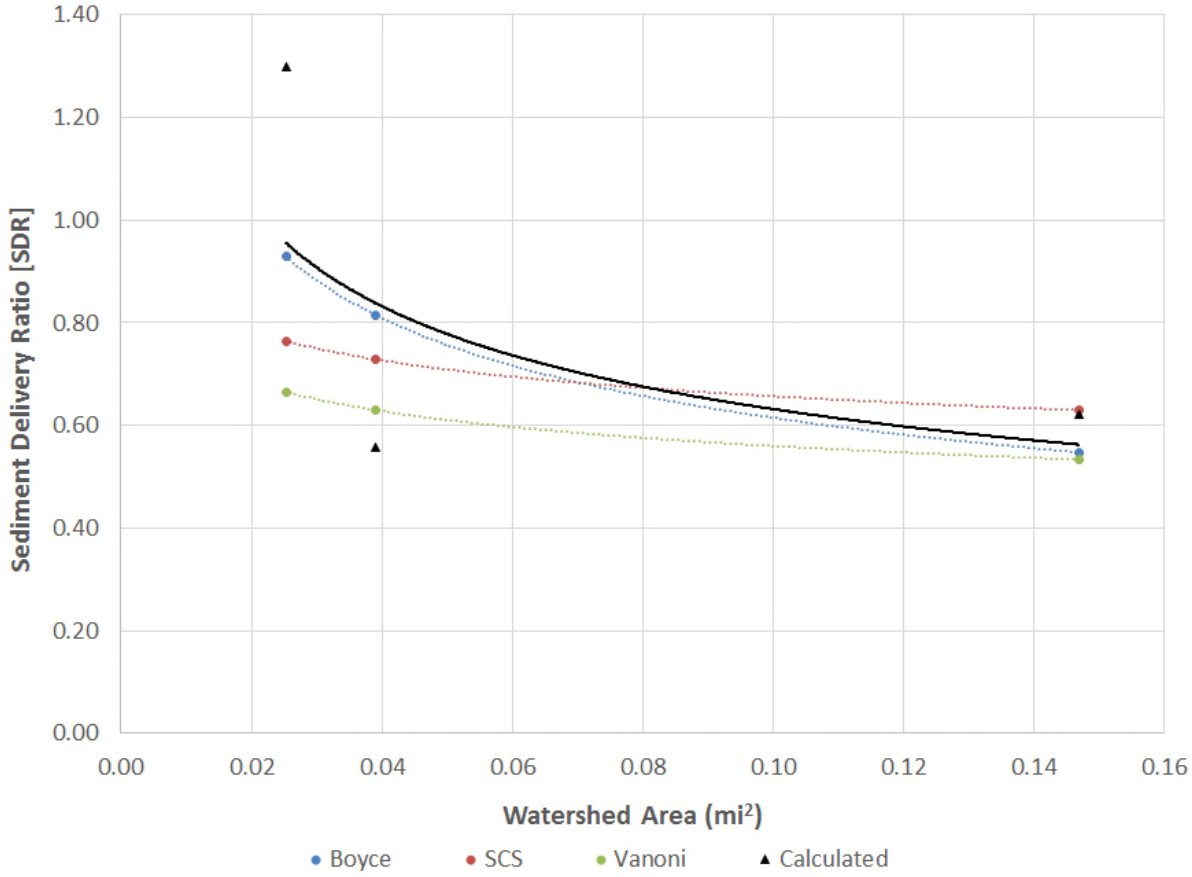

Figure 28 Sediment Delivery Ratio vs. Watershed Area

Overall, a similar decreasing trend is observed in watershed area and SDR value with the calculated and literature-reported values, and the calculated delivery ratios matched well with the literature-reported sediment delivery ratios.

5.3 SEDIMENT CONTAMINANT CONCENTRATIONS

The final objective of this study is to evaluate the sediment yield of the specific contaminants of concern (arsenic, uranium, and radium-226) using a combination of available soil contaminant mapping information and the results from the GIS based RUSLE model. The results of this aspect of the study were presented in Section 4.2.4. A validation was performed to assess the accuracy of these predicted downstream sediment concentrations. Historical data are available from previous geochemical characterization studies for arsenic, uranium, and radium-226.

Table 21 presents a comparison of the range and average arsenic concentrations measured in sediment ponds SP1, SP2, and SP3. The predicted arsenic concentration falls within the range of the measured arsenic concentrations for SP1 and SP2, and the average measured arsenic concentration matches closely with the predicted arsenic. The predicted arsenic concentration in sediment pond SP3 is 10 mg/kg higher than the average measured arsenic concentration in SP3.

Table 21 Summary of Observed and Predicted Arsenic Concentrations in Sediment Ponds

Sediment Pond ID	Observed Arsenic in Sediment			Predicted Arsenic in Sediment (mg/kg)
	Minimum (mg/kg)	Maximum (mg/kg)	Average (mg/kg)	
SP1	29	99	56	53
SP2	25	77	62	59
SP3	25	33	29	39

Table 22 presents a comparison of the range and average uranium concentrations measured in sediment ponds SP1, SP2, and SP3. The predicted arsenic concentration falls within the range of the measured uranium concentrations for all three sediment ponds.

Table 22 Summary of Observed and Predicted Uranium Concentrations in Sediment Ponds

Sediment Pond ID	Observed Uranium in Sediment			Predicted Uranium in Sediment (mg/kg)
	Minimum (mg/kg)	Maximum (mg/kg)	Average (mg/kg)	
SP1	3.2	21	10	12
SP2	11	26	16	12
SP3	3.1	36	12	11

Table 23 presents a comparison of the range and average radium-226 concentrations measured in sediment ponds SP1, SP2, and SP3. Only one data point was available for measured radium-226 concentrations in sediment for each pond. Overall, the predicted radium-226 concentrations are on the same order of magnitude as the observed concentrations.

Table 23 Summary of Observed and Predicted Radium-226 Concentrations in Sediment Ponds

Sediment Pond ID	Observed Radium-226 in Sediment (pCi/g)	Predicted Radium-226 in Sediment (pCi/g)
SP1	3.4	1.65
SP2	6.7	4.23
SP3	2.1	4.11

Overall, the predicted sediment concentrations matched well with the measured ranges and averages of arsenic, uranium, and radium-226 measured in the sediment ponds.

6.0 CONCLUSIONS

The degradation of land caused by strip mining is a multi-faceted phenomenon, where the effects seen are caused by deterioration of the land surface by accelerated removal of soil, progressive alteration of soil properties, and the loss of vegetative cover of the soil. Mining operations may introduce large volumes of sediment directly into natural streams, and these mine dumps and spoil banks often continue to erode by natural rainfall for many years after mining operations have ceased (Julien 2010), as is the case observed at the Riley Pass site. This site underwent severe strip mining for mineral extraction during the Cold War era uranium boom, and large volumes of contaminated sediment have been introduced to the surrounding streams many years after the mining operations ceased.

This study aimed to use a combination of statistically valid and innovative environmental double sampling techniques with soil loss and delivery ratio models in combination with modern GIS-based tools to estimate sediment yield and predicted sediment contaminant concentrations potentially draining from the study area. After terrain pre-processing of the study area was performed to identify watershed boundaries, a simple GIS-based application of the RUSLE model was applied using empirical and field observed data to predict gross erosion rates for each watershed draining the mine affected study area. The RUSLE model was implemented by using spatially distributed soil, vegetation, topographical and land use properties under a GIS environment. The sediment yield was estimated for each watershed using delivery ratio methods that rely on catchment size characteristics. The predicted sediment yield of each watershed was validated using measured sediment volumes. Overall, the predicted sediment yield was on the same order of magnitude as the measured sediment yield with acceptable tolerance on percent difference, further validating the RUSLE model and delivery ratio methods. The sediment delivery ratio was calculated using the results from the gross annual soil loss rates from the GIS-based RUSLE model and the measured sediment yield and resulted in delivery ratios within the general range of the values reported in technical literature.

The specific degradation of each watershed was then calculated for each watershed by relating sediment yield and catchment area. The results of this study show that the strip mining operations have had significant impacts on the Riley Pass site with erosion rates on average using the various delivery ratio methods as high as 6,396 metric tons/km^2-year (28.5 U.S. tons/acre-year), approximately 20 times higher than the median value that would be expected for an unimpacted watershed using literature reported values for the same size drainage area. Julien (2010) states that the erosion rates can range between 100 and 1,000 times greater than the natural geological erosion rate of 25 ton/km^2-year. The results of this analysis are not unexpected — for instance, in Kentucky a watershed with 10 percent of its area disturbed by active strip mining produced 57 times the sediment measured from a similar but undisturbed adjoining watershed (Collier et al., 1964). The percent disturbed area at the Riley Pass study area is much larger than 10 percent.

Finally, using the results from XRF field surveys and gamma radiation surveys, a geostatistical analysis was performed on the resultant contaminant data to generate GIS-based soil contaminant maps. The grid-based/GIS-based soil contaminant maps were combined with the GIS-based RUSLE gross erosion results and delivery ratio methods to estimate the predicted concentrations in sediment draining the watersheds of the study area. These predicted concentrations matched extremely well with observed contaminant concentrations for arsenic, uranium, and radium-226, further validating both the contaminant mapping and the erosion soil loss modeling.

The final results of this study showed the highest predicted sediment yield was observed in the South watershed (1,920 US tons/year) and the East watershed (1,097 US tons/year). However, the highest expected contaminant concentrations for arsenic, uranium, and radium-226 to occur downstream were all observed in the East watershed. The models showed that Southeast watershed had the highest specific degradation rate and second-highest expected contaminant concentrations for arsenic, uranium, and radium-226 downstream. Fortunately, a sediment pond was installed at interception point of the Southeast watershed already in 1989; however, no sediment pond has been installed to date at the interception point of the East watershed. The results of this study further validate the need for additional sediment controls in the East and North watersheds. The data presented in these evaluations do have engineering application potential for future sizing and placement design needs of watersheds within the study area, particularly at interception points downstream of the East watershed.

The models presented in this study are not without limitations; an important limitation to consider is that no corrections were added to take account of additional contributions from channel and gully erosion. However, for this analysis, the amount of contributing gully erosion is limited in comparison to sheet erosion expected to occur based on field observations. Additionally, the issue with spatial and temporal lumping presented in Walling (1983) is still a major factor when using delivery ratio methods that rely heavily on catchment size characteristics. Assessments that have been undertaken to develop a generally applicable delivery ratio prediction equation are themselves primarily based on a comparison of measured sediment yield with an estimate of gross erosion (Walling, 1983). The latter are generally derived from an estimate of sheet erosion based on a soil loss equation (such as RUSLE), which carries a certain amount of uncertainty itself. Lastly, a major assumption is that the parameters in the RUSLE model are not time variant and that static conditions are assessed, which may not be true based on potential seasonal variations affecting soil loss.

Overall, the results of this study were validated successfully within tolerable limits using available historical data. The validated model further emphasizes the importance of using soil loss modeling for sizing and prioritizing placement of engineered sediment control structures to prevent environmental degradation from heavy metals and radionuclide contamination into downstream natural streams and waterbodies. Additionally, using the combination of soil contaminant mapping with soil erosion modeling is a relatively new and unexplored technique that has significant potential within the assessment of abandoned uranium mining industry.

7.0 REFERENCES

Abelquist, E.W. (2001). Decommissioning Health Physics: A Handbook for MARSSIM Users Institute of Physics Publishing, 438p.

Aerometric. (2012). Airborne GPS Survey Report for the United States Geological Survey National Geospatial Technical Operations Center. *Mount Rushmore National Memorial and Riley Pass, Custer National Forest LiDAR.* Contract ID G10PC00025. Task Order G12PD01039. August.

Boggs, GS., Devonport, CC., Evans, KG., Saynor, MJ., Moliere, DR. (2001). Development of a GIS based approach to mining risk assessment. Supervising Scientist Report No. 159. Environment Australia.

Boyce, R. (1975). Sediment routing and sediment delivery ratios. In *Present and Prospective Technology for Predicting Sediment Yields and Sources,* USDA-ARS-S-40, pp. 61-65.

Collier, CR, et al. (1964). Influences of strip mining on the hydrologic environment of parts of Beaver Creek Basin, Kentucky. 1955-59. USGS Prof. Pap. 427-B, 85 p.

D.B., Huggins, L.F., and Monke, E.J. (1980). ANSWERS: a model for watershed planning. Transactions of the American Society of Agricultural Engineers 23: pp. 938–44.

Beasley, D.B., Huggins, L.F., and Monke, E.J. (1980). ANSWERS: a model for watershed planning. Transactions of the American Society of Agricultural Engineers 23: pp. 938–44.

D.B., Huggins, L.F., and Monke, E.J. (1980). ANSWERS: a model for watershed planning. Transactions of the American Society of Agricultural Engineers 23: pp. 938–44.

Das, B.M. (2000). *Fundamentals of Geotechnical Engineering*. Brooks/Cole, Pacific Grove. 24pp.

Curtiss, RE. (1955). A Preliminary Report on the Uranium in South Dakota. University of South Dakota, Vermillion, South Dakota. State Geological Survey ROI No. 79.

Environmental Science.org (ESO) (http://www.environmentalscience.org/) Website accessed July 19, 2015.

Fortuin, R. (2006). Soil Erosion in Cameron Highlands, an Erosion Rate Study of Highland Area. Saxion University Deventer.

Foster, G.R., McCool, K.G., Moldenhauer, W.C. (1981). Conversion of the universal soil loss equation to SI metric units. Journal of Soil and Water Conservation. November-December 1981. Volume 36. Number 6.

Gilbert, R.O. (1987). Statistical Methods for Environmental Pollution Monitoring, New York: John Wiley & Sons, Inc. 320 pp.

Glymph, LM., (1954). Studies of Sediment Yields of Watersheds. Publication No. 36, de L'Association International D'Hydrologie, International Union of Geodesy and Geophysics, 1954, pp. 178-191.

Goy, P.N. (2015). GIS-Based Soil Erosion Modeling and Sediment Yield of the N'Djili River Basin, Democratic Republic of Congo. Master's Science Thesis, Colorado State University. Fort Collins, Colorado.

Hua, L., Moran, CJ., Prosser, IP. (2006). Modelling Sediment Delivery Ratio over Murray Darling Basin. Supported by Murray Darling Basin Commission. CSIRO Land and Water. Australia.

Kim, H. (2006). Soil Erosion Modeling using RUSLE and GIS on the IMHA Watershed, Master's Science Thesis, Colorado State University. Fort Collins, Colorado.

Johnson, J.A., Meyer, H.R., Vidyasagar, M. (2006). Characterization of Surface Soils at a Former Uranium Mill. Health Physics 90 (Supplement 1): S29-S32, 2006.

Julien, P. Y. (2002). River Mechanics, Cambridge University Press, Cambridge, 454 p.

Julien, P. Y. (2010). Erosion and Sedimentation, 2nd ed. Cambridge University Press, Cambridge, 371 p.

Maner, SB., (1958). Factors Affecting Sediment Delivery Rates in the Red Hills Physiographic Area. Transactions, American Geophysical Union. Volume 39, Washington D.C., August, 1958, pp. 669-675.

Millward, A.A. and Mersey, J.E. (1999). Adapting the RUSLE to model soil erosion potential in a mountainous tropical watershed. Catena 38, 109-129.

Mitasova, H., Hofierka, J., Zlocha, M., and Iverson, R. (1996). Modeling Topographic Potential for Erosion and Deposition using GIS. In. Journal of Geographical Information Science 10 (5), 629-641.

Pelton, J., Frazier, E., Pickilingis, E. (2012). Calculating Slope Length Factor (LS) in the Revised Universal Soil Loss Equation (RUSLE) 2012

Portage Environmental, Inc. (2006). Final Human Health and Ecological Risk Assessment for the Riley Pass Uranium Mines in Harding County, South Dakota. Prepared for USDA Forest Service, Northern Regional Office. Portage. 88p.

South Dakota School of Mines and Technology (2007). Final Report: North Cave Hills Abandoned Uranium Mines Impact Investigation. Prepared for: U.S. Department of Agriculture Forest Service Region 1. Prepared by: Dr. James Stone, Dr. Larry Stetler, Dr. Albrecht Schwalm. April 18, 2007.

Robertson, A. MacG. (1996). The importance of site characterization for remediation of abandoned mine lands. Seminar Publication – Managing Environmental Problems at Inactive and Abandoned Mine Sites. United States Environmental Protection Agency, Washington D.C, October 1996.

Roehl, JW. (1962). Sediment Source Areas, Delivery Ratios and Influencing Morphological Factors. Publication 59, International Association of Scientific Hydrology, Commission of Land Erosion, 1962, pp. 202-213.

Renard K.G., Foster G.R., Weesies G.A, Porter J.P. (1991). RUSLE Revised universal soil loss equation. Journal of Soil and Water Conservation. January-February 1991, Volume 46, Number 1

Renard, K., Foster, G., Weesies, G., McDool, D., and Yoder, D. (1997). Predicting Soil Erosion by Water: A Guide to Conservation Planning with the Revised Universal Soil Loss Equation (RUSLE). Agricultural Handbook 703, USDA-ARS.

Rudra, R.P., Dickinson, W.T., and Wall, G.J. (1986). GAMES – a screening model of soil erosion and fluvial sedimentation on agricultural watersheds. Canadian Water Research Journal 11: 58–71.

Stone J.J., and Stetler L.D. (2009). Assessment of environmental impacts near abandoned uranium mines within the cave hills and slim buttes complexes, Custer National Forest, South Dakota. Proceedings of the American Society of Mining and Reclamation, Billings, MT. May 30 – June 5, 2009.

Toy, T.J., Foster, G.R. (1998). "Guidelines for the Use of the RUSLE Version 1.06 on Mined Lands, Construction Sites, and Reclaimed Lands. Office of Surface Mining and Reclamation (OSM) Denver, Colorado. August 1998.

Effect of biogeochemical redox processes on the fate and transport of As and U at an abandoned urnaium mine site: an X-ray absorption spectroscopy study." *Journal of Environmental Chemistry. Published online January 28,* 2014.

Troyer, L.D., Stone, J.J., Borch, T. (2014). "Effect of biogeochemical redox processes on the fate and transport of As and U at an abandoned urnaium mine site: an X-ray absorption spectroscopy study." *Journal of Environmental Chemistry. Published online January 28,* 2014.

United States Department of Agriculture[USDA]. (1986). Urban Hydrology for Small Watersheds. Technical Release 55 (TR-55), June 1986.

USDA. (1997). Agricultural Handbook Number 703: Predicting Soil Erosion by Water- A Guide to Conservation Planning with the Revised Universal Soil Loss Equation (RUSLE). Issued January 1997.

USDA. (2015). Web Soil Survey 2.0, National Cooperate Soil Survey, Harding County, South Dakota. http://websoilsurvey.sc.egov.usda.gov/. Accessed July 9, 2015.

U.S. Army Corps of Engineers (USACE). (2013). Hydrologic Modeling System (HEC-HMS) User's Manual, Version 4.0. December, 2013.

U.S. Department of Energy (DOE). (2014). Defense-Related Uranium Mines Assessment of Radiological Risk to Human Health and the Environment Topic Report. LMS/S11072. June 2014.

U.S. Environmental Protection Agency (EPA). (1989). Methods for Evaluating the Attainment of Cleanup Standards, Volume 1: Soils and Solid Media. EPA 230/02-89-042. February 1989.

EPA. (1995). Land Use in the CERCLA Remedy Selection Process [Memorandum]. OSWER No. 9355.7-04. May 25, 1995

EPA. (1996). An Overview of Methods for Evaluating the Attainment of Cleanup Standards for Soils, Solid Media, and Groundwater, EPA Volumes 1, 2, and 3. January 1996.

EPA. (1999). Establishment of Cleanup Levels for CERCLA Sites with Radioactive Contamination. OSWER No. 9200.4-18. [Memorandum]. August 22, 1999.

EPA. (2000). Abandoned Mine Site Characterization and Cleanup Handbook. EPA 910-B-00-001. August 2000.

EPA. (2008). Technical Report on TENORM from Uranium Mining Volume 2: Investigation of Potential Health, Geographic, And Environmental Issues of Abandoned Uranium Mines. EPA 402-R-05-007, August 2007. Revised April 2008.

U.S Department of Agriculture-Soil Conservation Service [USDA-SCS]. (1979). United States Department of Agriculture - Soil Conservation Service. National Engineering Handbook, Sec. 4. Hydrology.

U.S. Forest Service (USFS). (2004) Recommendation for An Action Memorandum: Time Critical Removal Action at Riley Pass Abandoned Uranium Mine Harding County, South Dakota. File Code 2160/6740/2840. September 7, 2004.

USFS. (2006). Riley Pass Uranium Mines Site, Final Engineering Evaluation/Cost Analysis, Prepared by Pioneer Technical Services Inc. for the U.S. Department of Agriculture/Forest Service Region 1, Custer National Forest, Sioux Ranger District, Harding County, South Dakota. November, 2006.

USFS. (2007). Riley Pass Uranium Mines Site Removal Action, Action Memorandum, Custer National Forest, Sioux Ranger District, Harding County, South Dakota. February.

USFS. (2010). Riley Pass Uranium Mines Site Non-Tronox Bluffs Removal Action, Action Memorandum, Custer National Forest, Sioux Ranger District, Harding County, South Dakota. April, 2010.

U.S. Nuclear Regulatory Commission (NRC). (1994). NUREG-1501, Background as a Residual Radioactivity Criterion for Decommissioning, Date Published: August 1994, Prepared by A.M. Huffert, R.A. Meck, K.M. Miller.

NRC. (2000). Multi-Agency Radiation Survey and Site Investigation Manual (MARSSIM), (NUREG 1575, Revision 1). NRC. 360p.

Van Remortel R., Hamilton M., Hickey R. (2001). "Estimating the LS Factor for RUSLE through Iterative Slope Length Processing of Digital Elevation Data within ArcInfo Grid," *Cartography,* vol. 30, no. 1, pp. 27-35.

Vanoni, V. A., ed. (1975). Sedimentation engineering. Manual 54, American Society of Civil Engineers, New York, 745 p.

Vitkus, T.J., Bailey, E.N. (2007). Advantages and lessons learned using GPS-enabled gamma scanning for the characterization survey of a large thorium/uranum site. Proceedings of the Healthy Physics Society Mid-Year Meeting, Knoxville, Tennessee. McLean, Virginia: Health Physics Society.

Anton, JJ., Rompaey, V., Verstraeten, G., Van Oost, K., Govers, G., Poesen, J. (2001) Modelling Mean Annual Sediment Yield Using a Distributed Approach. Earth Surface Processes and Landforms. Volume 26. 1221-1236. June 18, 2001.

Remortel R., Hamilton M., Hickey R. (2001) "Estimating the LS Factor for RUSLE through Iterative Slope Length Processing of Digital Elevation Data within ArcInfo Grid," *Cartography,* vol. 30, no. 1, pp. 27-35, 2001.

Wang, X. & Yin, Z.Y. (1997). An evaluation of Using ArcInfo to Extract Basin Physiographic Parameters from DEMs. In: ESRI INTERNATIONAL USER CONFERENCE, 1997, San Diego, Proceedings … ESRI, San Diego. Available at: . Accessed in: 2 May 2006

Walling, D.E, (1983) The sediment delivery problem. In: I. Rodriquez-Iturbe and V.K. Gupta (Guest-Editors), Scale Problems in Hydrology. J. Hydrol., 65: 209-237. Accepted for publication July 13, 1982

Whicker, R., Cartier, P., Cain, J., Milmine, K. and Griffin, M. (2008) Radiological site characterizations: gamma surveys, gamma/radium-226 correlations, and related spatial analysis techniques, The Radiation Safety Journal S180. November.

Whicker, R., D., Chambers, (2015) Normalization of Energy-Dependent Gamma Survey Data The Radiation Safety Journal Volume 108 No. 5. May.

Wischmeier, WH., Smith, DD. (1958). Rainfall Energy and Its Relationship to Soil Loss. *Transactions*, American Geophysical Union, Vol. 39, Washington D.C., 1958 pp. 285-291.

Wischmeier, WH., Smith, DD. (1962). Storms and soil conservation . J. Soil and Water Conservation. 17:55-59